Robust guiding and control of light and sound in photonic and acoustic metamaterials

Alexander B. Khanikaev[1,2]

[1]Electrical Engineering and Physics, City College of New York,

[2]Physics Department, Graduate Center of CUNY;

Collaborators: Andrea Alu, UT Austin
Yuri Kivshar, ANU

Mathematical & Physical Aspects of Topologically Protected States, Columbia University, May 1-3, 2017

Topological roadmap:
From Quantum Hall effect to Topological insulators

Broken TR symmetry

$$H = H_0 - \mu_B \boldsymbol{S} \cdot \boldsymbol{B}$$

One-way edge states

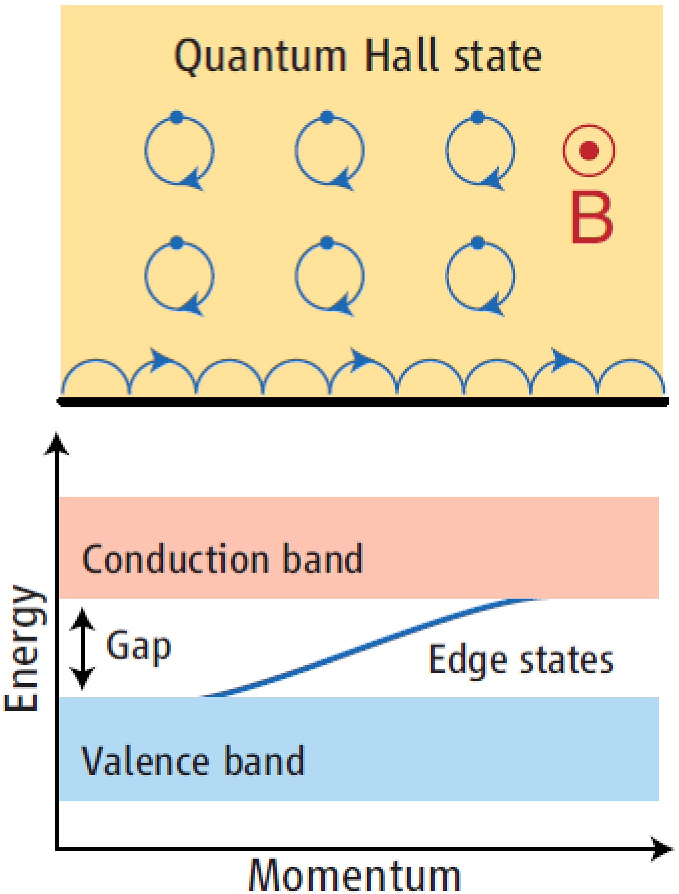

v. Klitzing, *Phys. Rev. Lett.* **45**, 494 (1980).
Nobel prize 1985

All the advantages of topological protection without magnetic bias!

25 years apart

Robust edge states in the gap

Preserved TR symmetry

$$H = H_0 - \chi_{SO} \boldsymbol{S} \cdot \boldsymbol{L}$$

Spin-locked one-way edge states

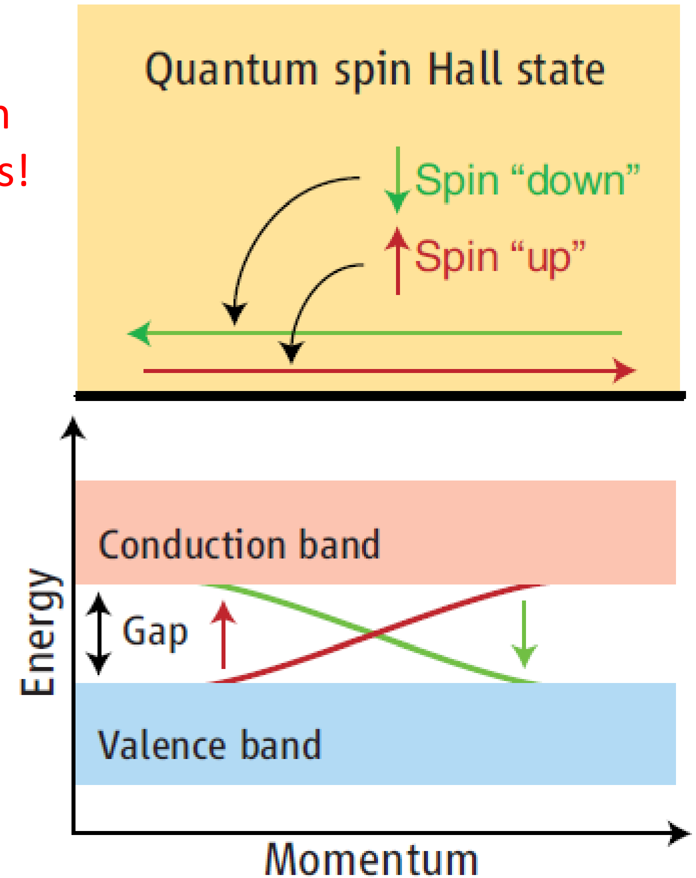

Kane, C. L. & Mele, E. J.,
Phys. Rev. Lett. **95**, 146802 (2005).

From condensed matter to photonics: photonic crystals – semiconductors of light

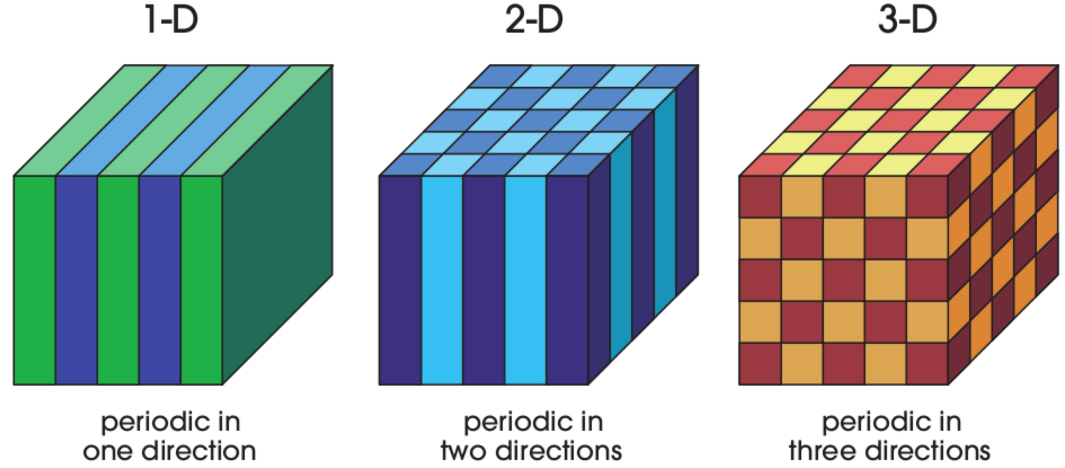

Joannopoulos, J. D., Johnson, S. G., Winn, J. N. & Meade, R. D., *Photonic Crystals: Molding the Flow of Light*, 2nd ed. (Princeton University Press, Princeton , 2008).

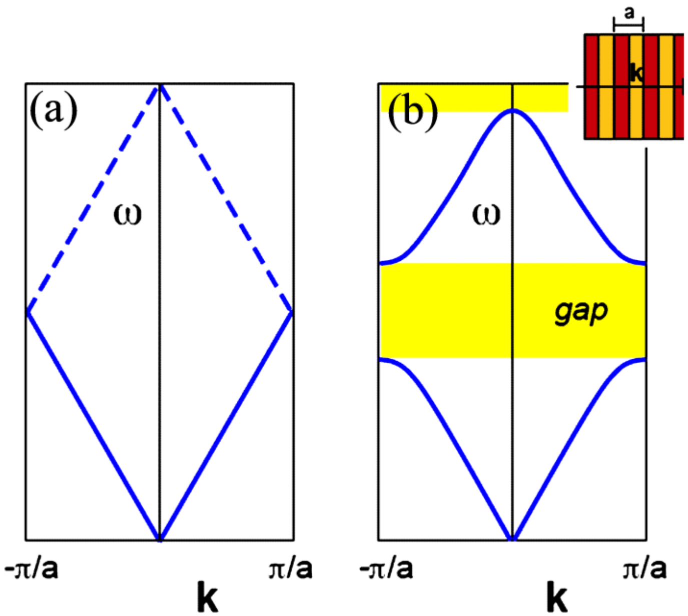

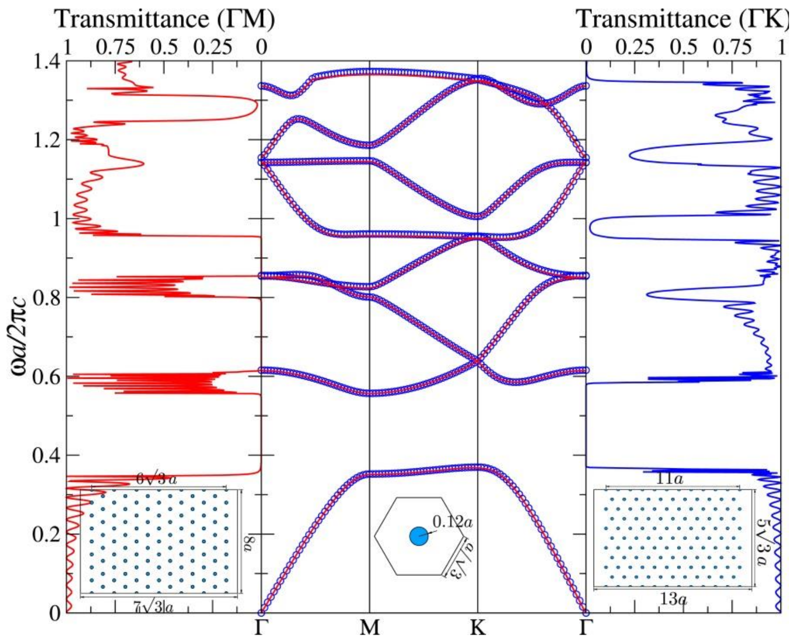

Topological order for photons

Broken TR symmetry and Floquet

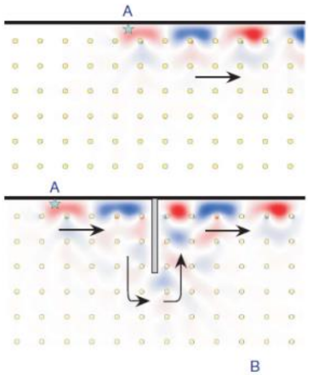

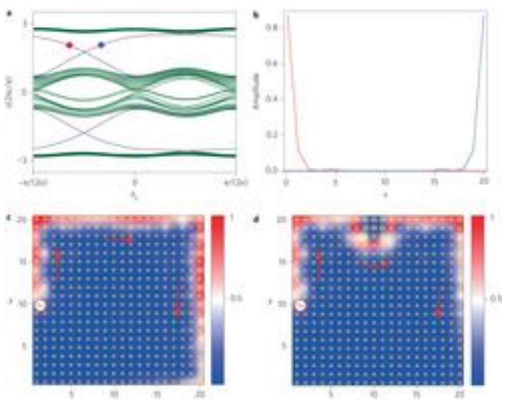

PRL **100**, 013904, (2008)
Nature 461, 772-775 (2009). *Nature Photon.* 6, 782–787 (2012)

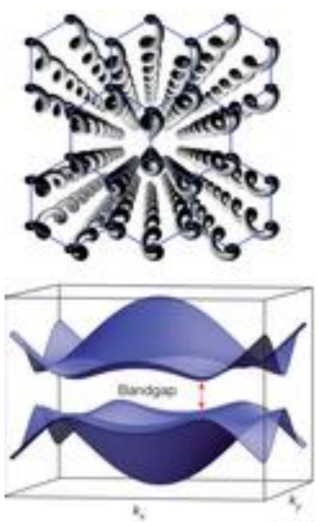

Nature 496, 196–200, (2013)

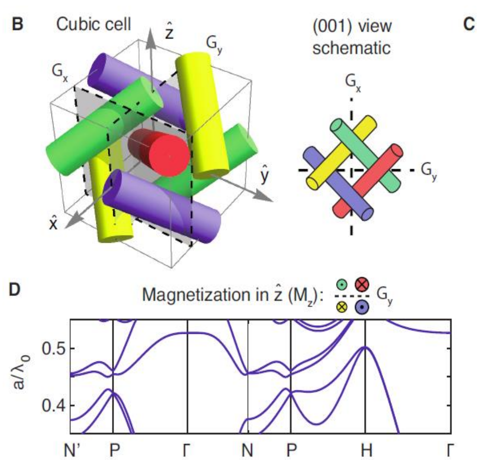

arXiv:1507.00337 (2015)
Nature Physics (2016)

Preserved TR symmetry

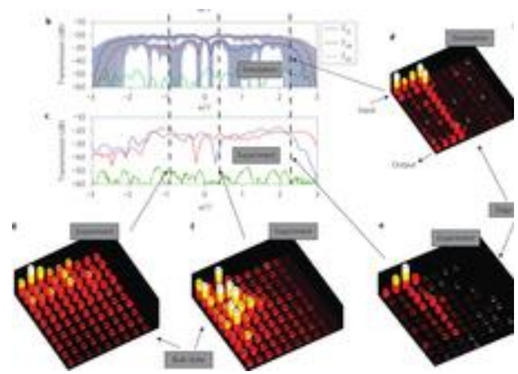

Nature Phys. **7**, 907–912 (2011).
Nature Photon. **7**, 1001–1005 (2013)

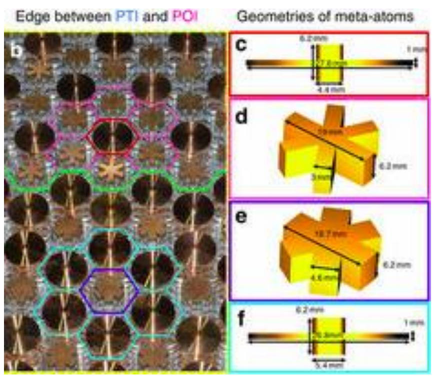

Nature Comm. 5, 5782, (2014)

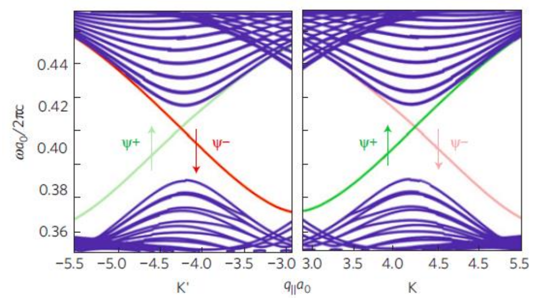

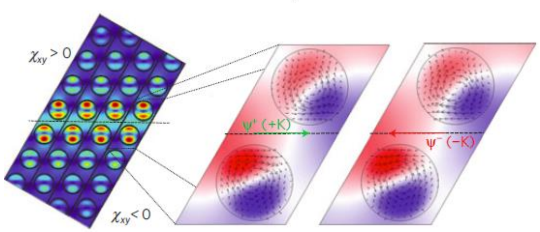

arXiv:1401.1276 (2012)
Nature Mater. **12**, 233–239 (2012)

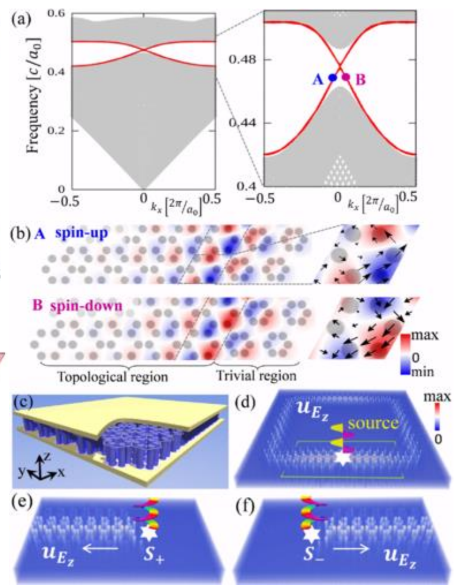

Phys. Rev. Lett. **114**, 223901 (2015)

Analogue of Quantum Hall Effect: One-Way Edge States in 2D Magnetic PC

Bulk

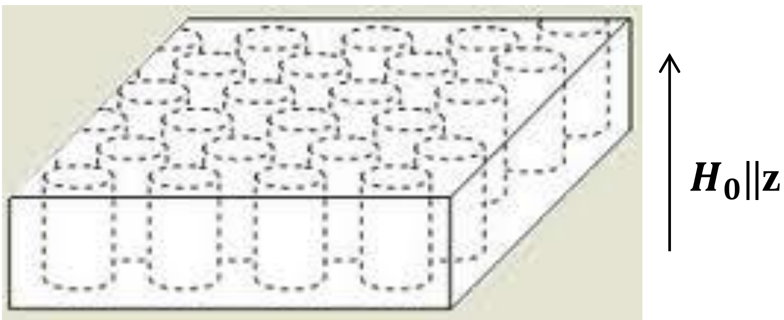

Edge

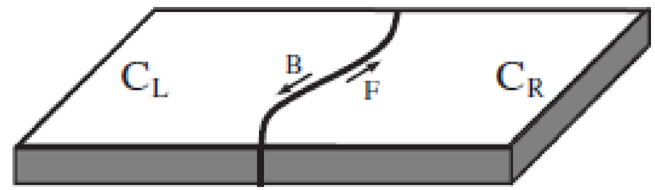

The number of forward-minus the number of backward-moving edge modes equals the difference of the Chern number of the band across the interface.

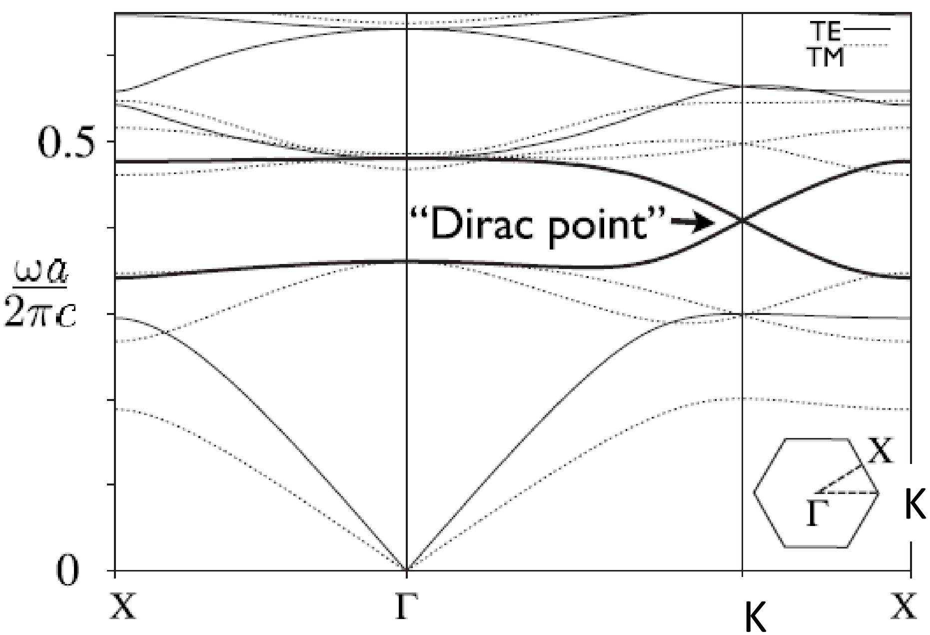

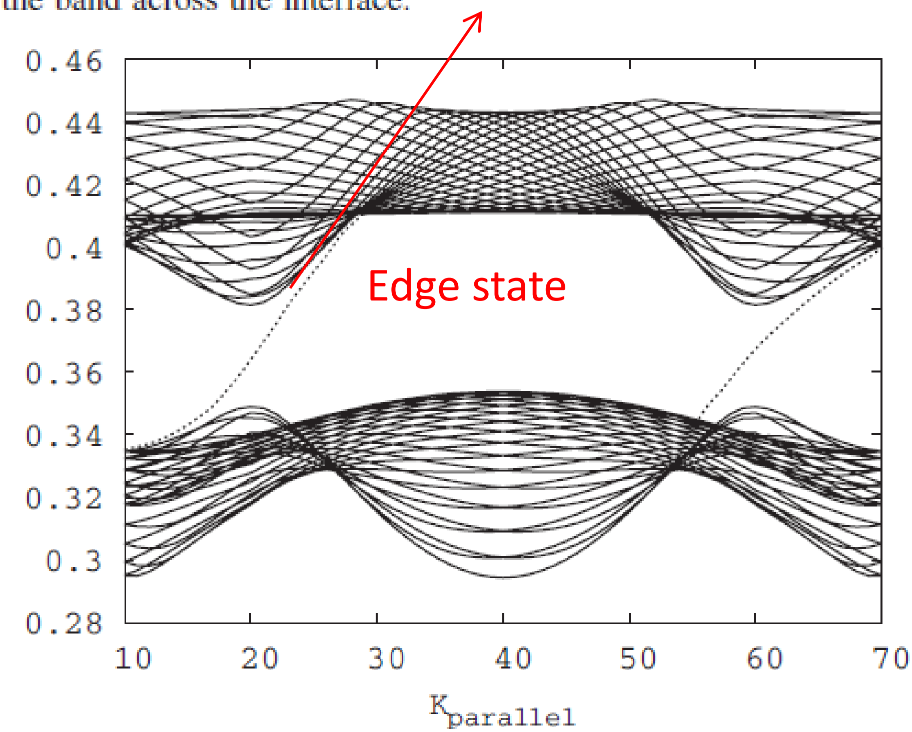

Raghu, S. & Haldane, F. D. M., *Phys. Rev. A* **78**, 033834 (2008)

Topological order for photons

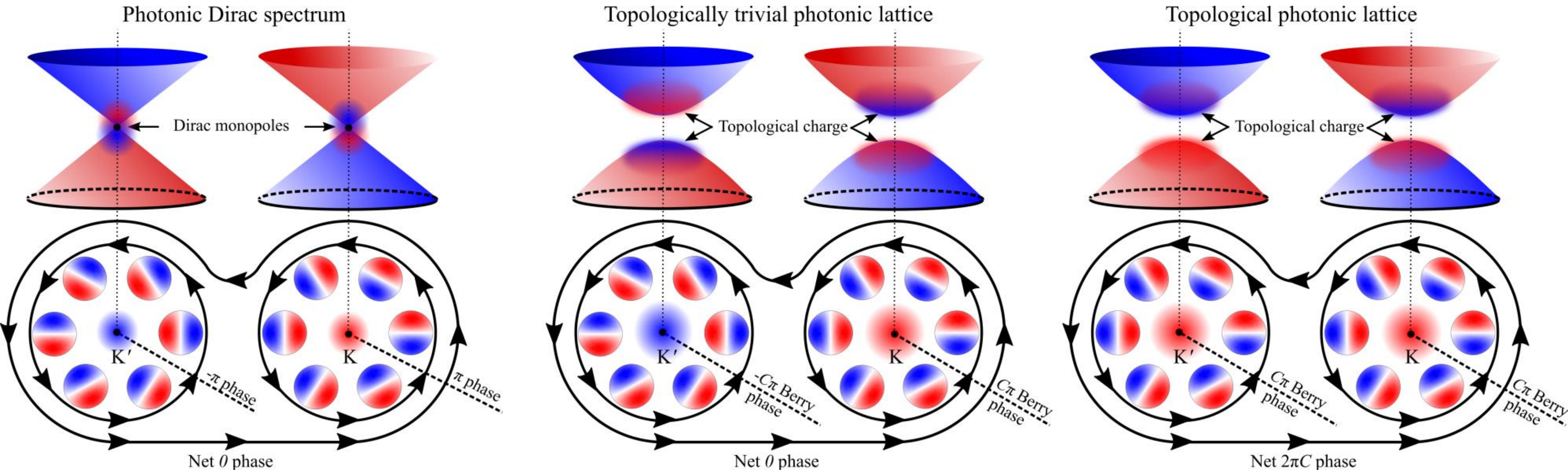

Bulk

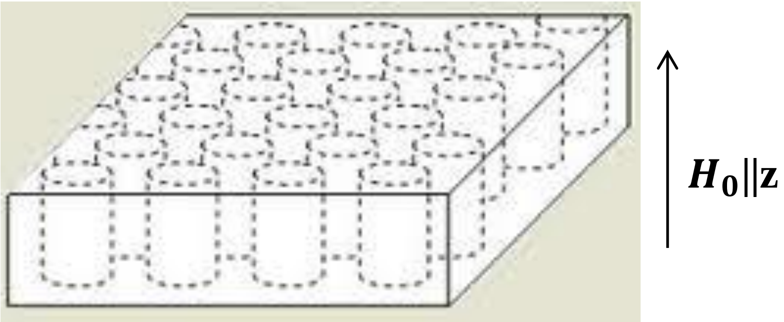

$$\{-[\nabla + i\tilde{\mathbf{A}}(\mathbf{r})]^2 + \tilde{V}(\mathbf{r})\}\psi(\mathbf{r}) = 0$$

$$\tilde{\mathbf{A}} = \tilde{\mu}/2[\nabla \times \tilde{\eta}(\mathbf{r})]\hat{\mathbf{z}}$$

$$\mathcal{A}(\mathbf{k}) = \langle\psi(\mathbf{r})|\nabla_k|\psi(\mathbf{r})\rangle$$

$$C = \frac{1}{2\pi i}\int_{\mathrm{BZ}} d^2k[\nabla_k \times \mathcal{A}]_z$$

Topological order for photons

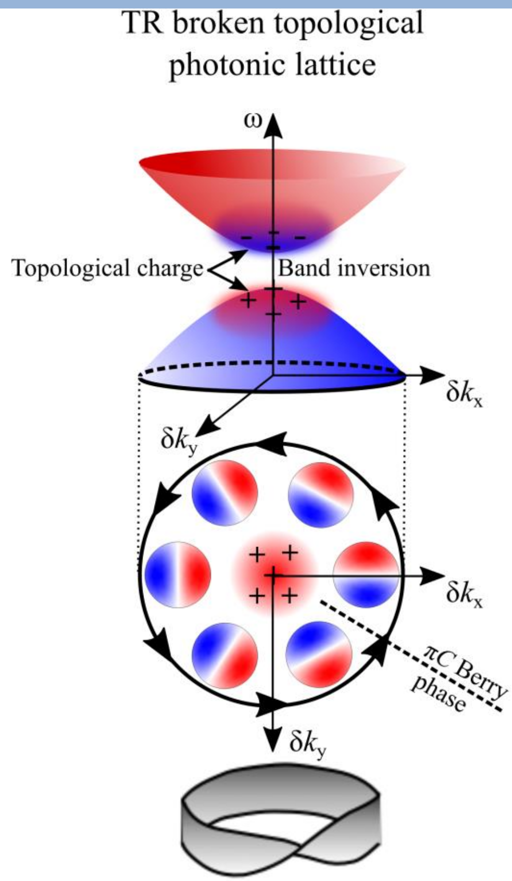

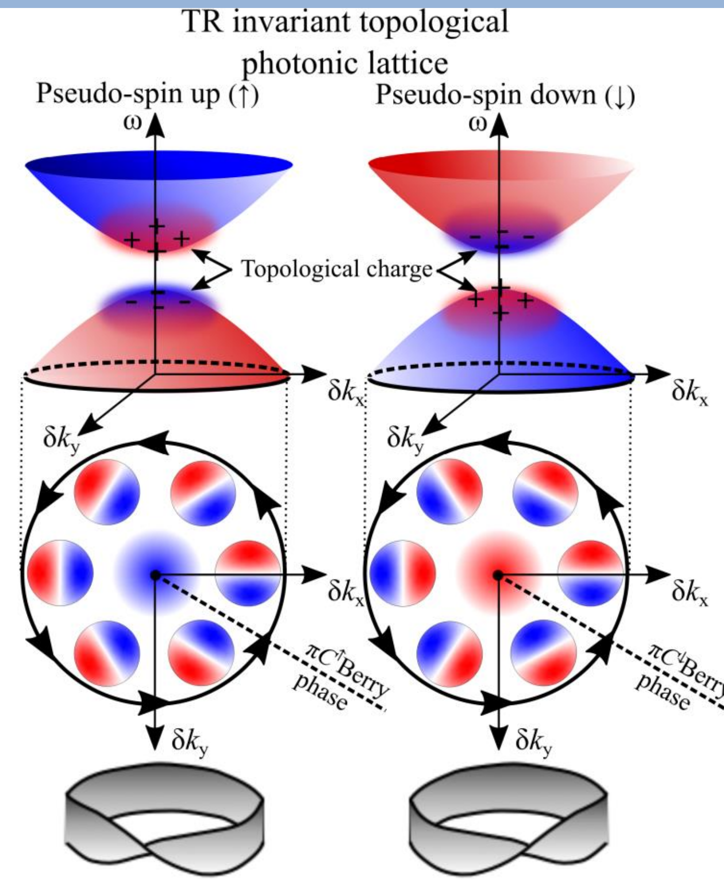

$$\{-[\nabla + i\widetilde{\mathbf{A}}(\mathbf{r})]^2 + \tilde{V}(\mathbf{r})\}\psi(\mathbf{r}) = 0$$

$$\widetilde{\mathbf{A}} = \tilde{\mu}/2[\nabla \times \tilde{\eta}(\mathbf{r})]\hat{\mathbf{z}}$$

$$\mathcal{A}(\mathbf{k}) = \langle\psi(\mathbf{r})|\nabla_k|\psi(\mathbf{r})\rangle$$

$$C = \frac{1}{2\pi i}\int_{\mathrm{BZ}} d^2k[\nabla_k \times \mathcal{A}]_z$$

$$\{-[\nabla \pm i\widetilde{\mathbf{A}}(\mathbf{r})]^2 + \tilde{V}^{\uparrow(\downarrow)}(\mathbf{r})\}\psi^{\uparrow(\downarrow)}(\mathbf{r}) = 0$$

$$\widetilde{\mathbf{A}} = \tilde{\mu}/2[\nabla \times \tilde{\zeta}(\mathbf{r})]\hat{\mathbf{z}}$$

$$\mathcal{A}^{\uparrow(\downarrow)}(\mathbf{k}) = \langle\psi^{\uparrow(\downarrow)}(\mathbf{r})|\nabla_k|\psi^{\uparrow(\downarrow)}(\mathbf{r})\rangle$$

$$C^{\uparrow(\downarrow)} = \frac{1}{2\pi i}\int_{\mathrm{BZ}} d^2k\left[\nabla_k \times \mathcal{A}^{\uparrow(\downarrow)}\right]_z$$

Topological order for photons

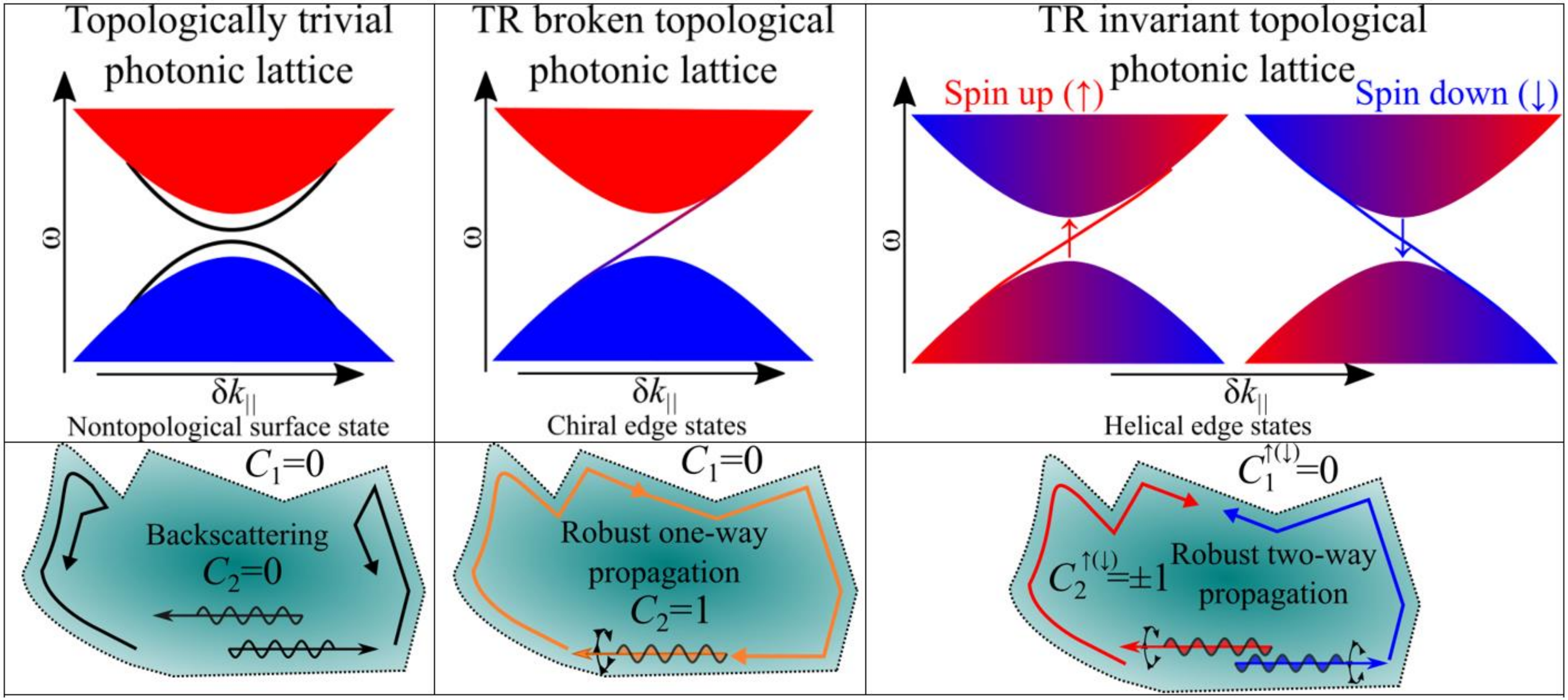

Role of Symmetry and Gauge Potentials in Topological Phases

Preserved TR symmetry ensures the presence of Kramer's TR partners (two spins/helicities) in fermionic systems but not in bosonic.

Fermions

$$\hat{\mathcal{H}} = \hat{\mathcal{H}}_0 + \hat{V}_{SO}$$

$\hat{\mathcal{H}}_0$ - unperturbed fermionic lattice potential

$\hat{V}_{SO} = -\chi_{SO}\hat{\boldsymbol{S}} \cdot \hat{\boldsymbol{L}}$ - gauge (SO) potential inducing topological transition (band crossing)

$$\hat{\mathcal{T}}_f \hat{\mathcal{H}} \hat{\mathcal{T}}_f^{-1} = \hat{\mathcal{H}} \text{ and } \hat{\mathcal{T}}_f^2 = -1$$

Robustness is insured by TR symmetry (no magnetic defects are allowed). Doublets generated by TR are locked to their propagation directions – **spin-locking.**

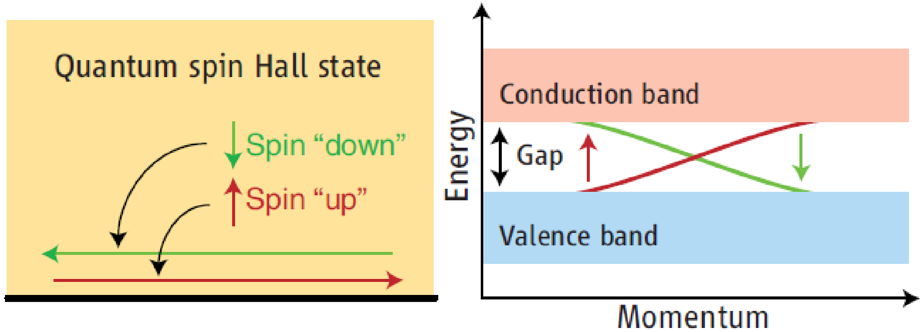

Kane, C. L. & Mele, E. J., *Phys. Rev. Lett.* **95**, 146802 (2005).
Hasan, M. Z. & Kane, C. L., Rev. Mod. Phys. 82, 3045-3067 (2010).
Qi, X.-L. & Zhang, S.-C., Rev. Mod. Phys. 83, 1057-1110 (2011).

Classical/Bosons

$$\hat{\mathcal{H}} = \hat{\mathcal{H}}_0 + \hat{V}_{gauge}$$

$\hat{\mathcal{H}}_0$ - unperturbed bosonic lattice potential

$\hat{V}_{gauge}$ =**Photonic** gauge potential (SO or pseudo-magnetic) inducing topological transition

$$\hat{\mathcal{T}}_b \hat{\mathcal{H}} \hat{\mathcal{T}}_b^{-1} = \hat{\mathcal{H}} \text{ and } \hat{\mathcal{T}}_b^2 = 1$$

Consequence: TR alone is not sufficient for topological order for bosons, i.e. no topological phase analogous to fermionic TR phase is possible.

Solution: non-TR symmetry protected phases.

$$\hat{C}_b \hat{\mathcal{H}} \hat{C}_b^{-1} = \hat{\mathcal{H}} \text{ and } \hat{C}_b^2 = -1$$

Where $\hat{C}_b$ is a spatial or internal symmetry operator generating a doublet state – **pseudo-spin degree of freedom**.

$$\hat{\mathcal{T}}_b \psi^{\uparrow(\downarrow)}(\boldsymbol{k}) = \hat{\mathcal{T}}_b \psi^{\downarrow(\uparrow)}(-\boldsymbol{k})$$

Role of Symmetry and Gauge Potentials in Topological Phases

Photonic topological insulator:

I. Duality of EM field as the pseudo-spin generating symmetry

Duality in free space follows by the symmetry of Maxwell equations with respect to electric and magnetic fields: $\hat{D}(\boldsymbol{E},\boldsymbol{H}) \rightarrow (-\boldsymbol{H},\boldsymbol{E})$

Broken by materials response $\hat{\epsilon} \neq \hat{\mu}$, it can be restored by (meta-)material's design.

In dual material $\epsilon_{zz} = \mu_{zz}$, $\epsilon_{\perp} = \mu_{\perp}$, duality transformation operator, which satisfies $\hat{D}^2 = -1$, allows emulating spin degree of freedom.

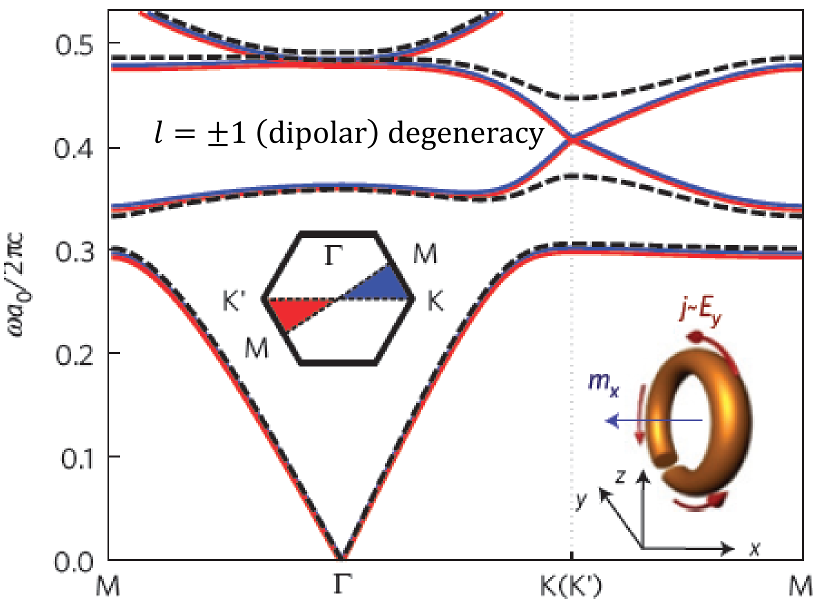

Khanikaev *et al.*, Nat. Mater. **12**, 233 (2012).

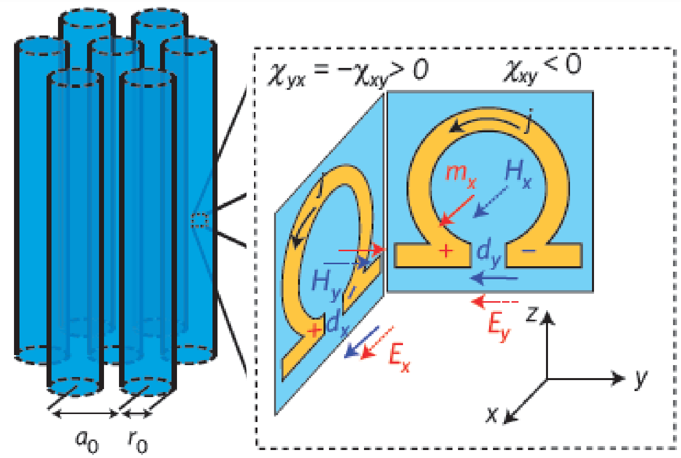

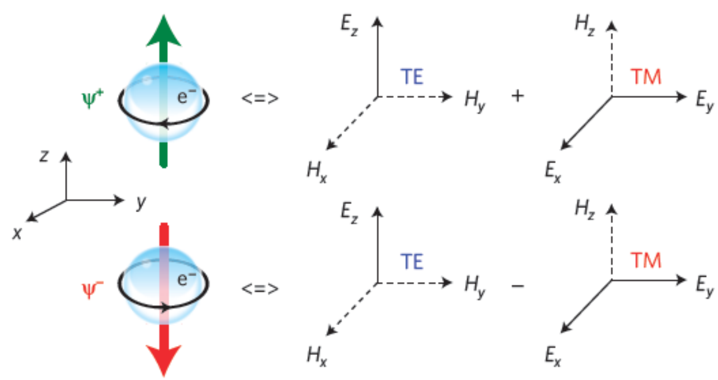

$$\psi^{\pm}(\boldsymbol{r};\boldsymbol{k}) = E_z(\boldsymbol{r};\boldsymbol{k}) \pm H_z(\boldsymbol{r};\boldsymbol{k})$$

$$\hat{\mathcal{T}}_b\, \psi^{\pm}(\boldsymbol{r};\boldsymbol{k}) = \psi^{\mp}(\boldsymbol{r};-\boldsymbol{k})$$

Role of Symmetry and Gauge Potentials in Topological Phases

Photonic topological insulator:

II. Bianisotropy as the gauge field

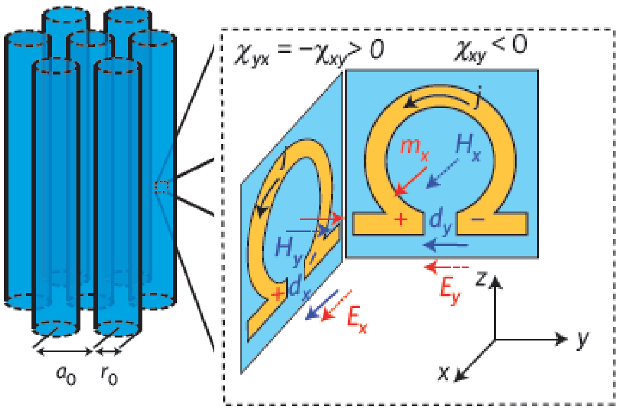

$$\boldsymbol{D} = \hat{\epsilon}\boldsymbol{E} + i\hat{\chi}\boldsymbol{H} \text{ and } \boldsymbol{B} = \hat{\mu}\boldsymbol{H} - i\hat{\chi}^T\boldsymbol{E}, \text{ where } \hat{\chi} = \begin{pmatrix} 0 & \chi & 0 \\ -\chi & 0 & 0 \\ 0 & 0 & 0 \end{pmatrix}$$

$$\hat{\mathcal{H}} = v_D \hat{\tau}_0 \hat{s}_0 \hat{\boldsymbol{\sigma}}_{\parallel} \cdot \delta \boldsymbol{k}_{\parallel} + m \hat{\tau}_3 \hat{s}_3 \hat{\sigma}_3$$

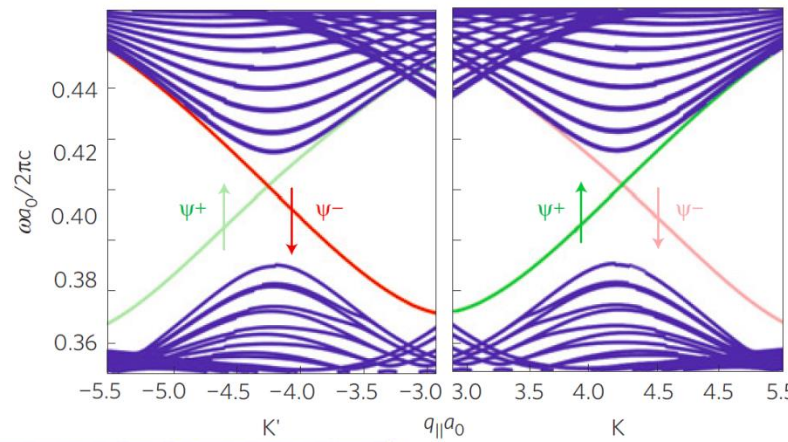

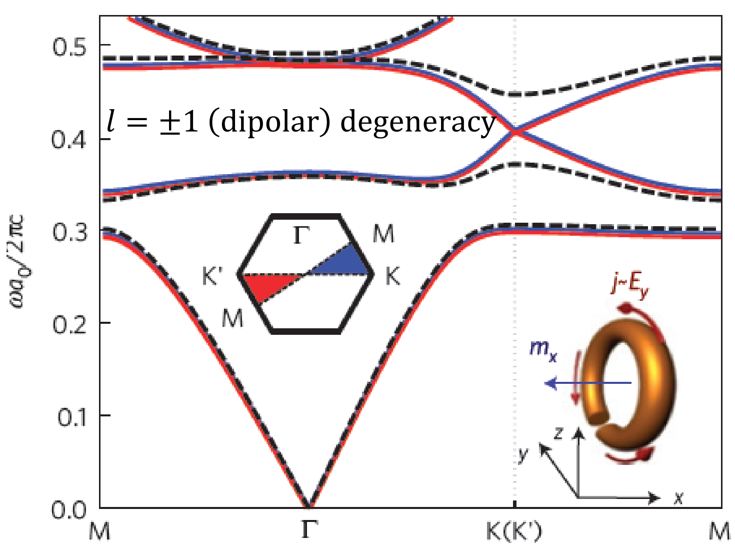

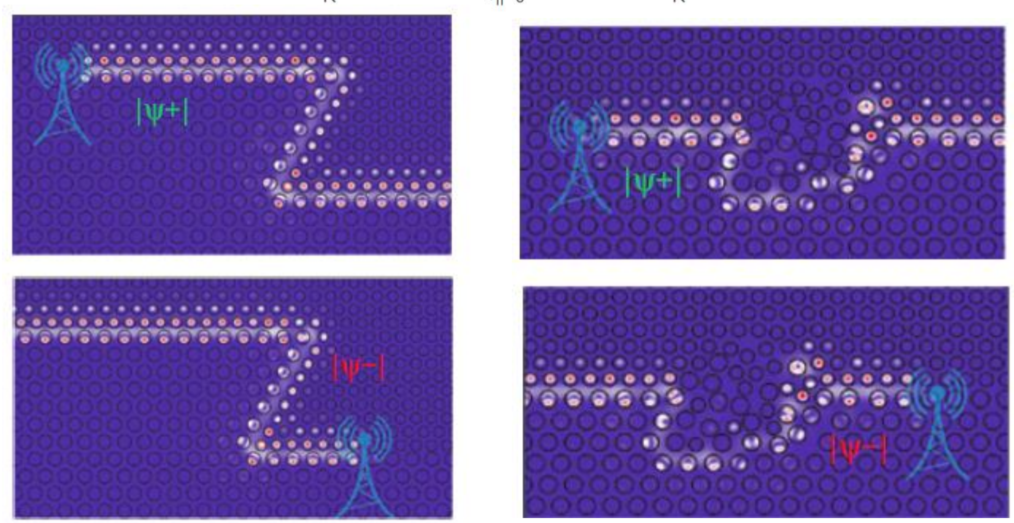

Khanikaev *et al.*, Nat. Mater. **12**, 233 (2012).

Topological Order in Metamaterials

Known approach: gyroelectric $\boldsymbol{D} = \hat{\epsilon}\boldsymbol{E}$ **or gyromagnetic response** $\boldsymbol{B} = \hat{\mu}\boldsymbol{H}$

$$\begin{pmatrix} 0 & \nabla \times \\ -\nabla \times & 0 \end{pmatrix} \begin{pmatrix} \boldsymbol{E} \\ \boldsymbol{H} \end{pmatrix} = \frac{i\omega}{c} \begin{pmatrix} \hat{\epsilon} & 0 \\ 0 & \hat{\mu} \end{pmatrix} \begin{pmatrix} \boldsymbol{E} \\ \boldsymbol{H} \end{pmatrix}$$

Our approach: bianisotropy or magneto-electric coupling*

More general constitutive relations $\boldsymbol{D} = \hat{\epsilon}\boldsymbol{E} + (\hat{\chi} - i\hat{\kappa})\boldsymbol{H}$ and $\boldsymbol{B} = \hat{\mu}\boldsymbol{H} + (\hat{\chi}^T + i\hat{\kappa})\boldsymbol{E}$

$$\begin{pmatrix} 0 & \nabla \times \\ -\nabla \times & 0 \end{pmatrix} \begin{pmatrix} \boldsymbol{E} \\ \boldsymbol{H} \end{pmatrix} = \frac{i\omega}{c} \begin{pmatrix} \hat{\epsilon} & \hat{\chi} - i\hat{\kappa} \\ \hat{\chi}^T + i\hat{\kappa} & \hat{\mu} \end{pmatrix} \begin{pmatrix} \boldsymbol{E} \\ \boldsymbol{H} \end{pmatrix}$$

Bi-isotropic materials
(chiral molecules, subwavelength helixes)

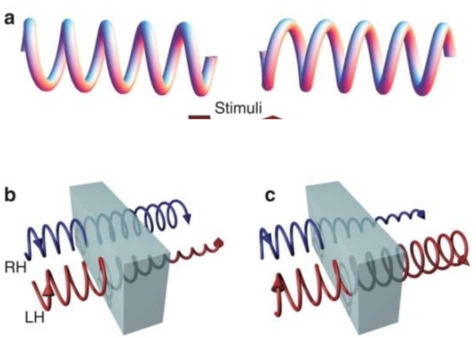

$$\hat{\kappa} = \begin{pmatrix} \alpha & 0 & 0 \\ 0 & \alpha & 0 \\ 0 & 0 & \alpha \end{pmatrix}$$

Bi-anisotropic materials/metamaterials (split-rings and Ω-particles)

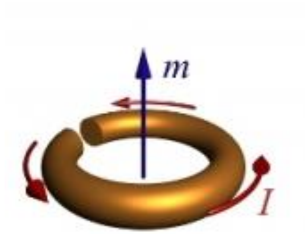

$$\hat{\kappa} = \begin{pmatrix} 0 & \kappa & 0 \\ -\kappa & 0 & 0 \\ 0 & 0 & 0 \end{pmatrix}$$

*A.N. Serdyukov, I.V. Semchenko, S.A. Tretyakov, A. Sihvola, *Electromagnetics of bi-anisotropic materials: Theory and applications,* 2001

QSHE as two copies of QHE in electromagnetic systems

Pseudo-gyroelectric + pseudo-gyromagnetic

More general constitutive relations $\boldsymbol{D} = \hat{\epsilon}\boldsymbol{E} + i\hat{\chi}\boldsymbol{H}$ and $\boldsymbol{B} = \hat{\mu}\boldsymbol{H} - i\hat{\chi}^T\boldsymbol{E}$

$$\begin{pmatrix} 0 & \boldsymbol{\nabla}\times \\ -\boldsymbol{\nabla}\times & 0 \end{pmatrix}\begin{pmatrix} \boldsymbol{E} \\ \boldsymbol{H} \end{pmatrix} = \frac{i\omega}{c}\begin{pmatrix} \hat{\epsilon} & i\hat{\chi} \\ -i\hat{\chi}^T & \hat{\mu} \end{pmatrix}\begin{pmatrix} \boldsymbol{E} \\ \boldsymbol{H} \end{pmatrix}$$

Bianisotropic metamaterials (split-rings and Ω-particles)

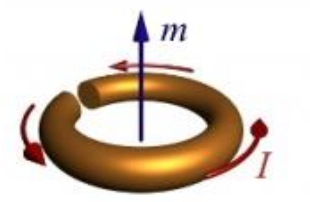

$$\hat{\chi} = \begin{pmatrix} 0 & \chi & 0 \\ -\chi & 0 & 0 \\ 0 & 0 & 0 \end{pmatrix} \qquad \begin{pmatrix} 0 & \boldsymbol{\nabla}\times \\ -\boldsymbol{\nabla}\times & 0 \end{pmatrix}\begin{pmatrix} \boldsymbol{E} \\ \boldsymbol{H} \end{pmatrix} = \frac{i\omega}{c}\begin{pmatrix} \hat{\epsilon} & i\hat{\chi} \\ i\hat{\chi} & \hat{\mu} \end{pmatrix}\begin{pmatrix} \boldsymbol{E} \\ \boldsymbol{H} \end{pmatrix}$$

If $\hat{\epsilon} = \hat{\mu}$ after simple transformation $\boldsymbol{\psi}^+ = \boldsymbol{E} + \boldsymbol{H}$ and $\boldsymbol{\psi}^- = \boldsymbol{E} - \boldsymbol{H}$

$$\begin{pmatrix} 0 & -\boldsymbol{\nabla}\times \\ \boldsymbol{\nabla}\times & 0 \end{pmatrix}\begin{pmatrix} \boldsymbol{\psi}^+ \\ \boldsymbol{\psi}^- \end{pmatrix} = i\omega\begin{pmatrix} \hat{\epsilon} + i\hat{\chi} & 0 \\ 0 & \hat{\mu} - i\hat{\chi} \end{pmatrix}\begin{pmatrix} \boldsymbol{\psi}^+ \\ \boldsymbol{\psi}^- \end{pmatrix}$$

Which are exact **two copies** of electromagnetic QHE for $\boldsymbol{\psi}^+$ and $\boldsymbol{\psi}^-$
with **inverted effective magnetic fields**

$$\boldsymbol{\psi}^+ : \hat{\epsilon} + i\hat{\chi} = \begin{pmatrix} \epsilon_{xx} & i\chi & 0 \\ -i\chi & \epsilon_{yy} & 0 \\ 0 & 0 & \epsilon_{zz} \end{pmatrix} \qquad \boldsymbol{\psi}^- : \hat{\epsilon} - i\hat{\chi} = \begin{pmatrix} \epsilon_{xx} & -i\chi & 0 \\ i\chi & \epsilon_{yy} & 0 \\ 0 & 0 & \epsilon_{zz} \end{pmatrix}$$

Quantum Spin Hall Effect in Metamaterials

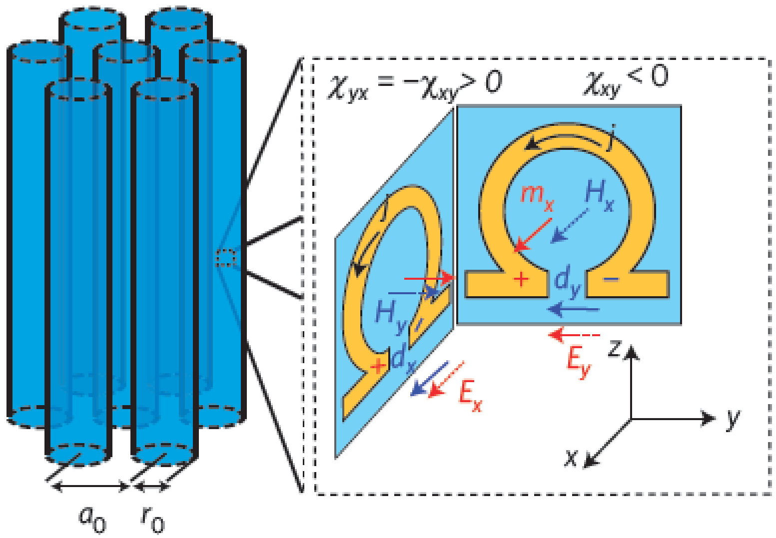

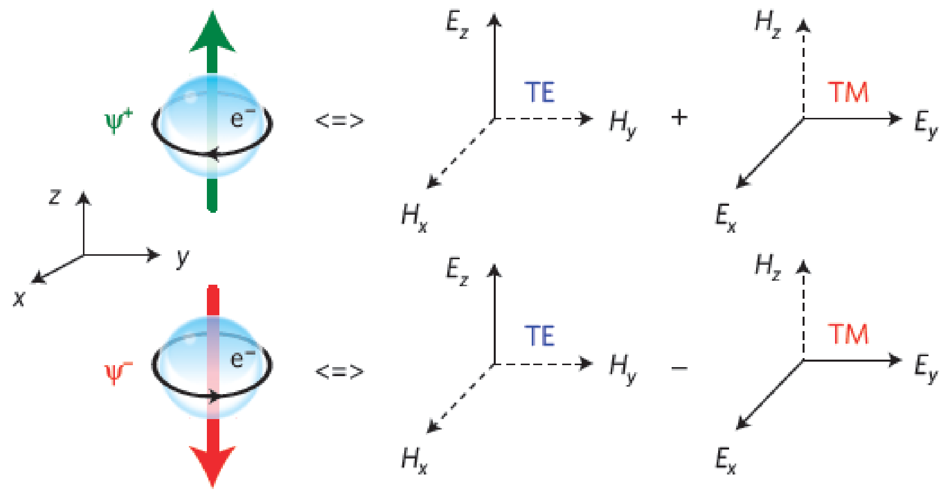

2-D Meta-Crystal: Photonic Crystal comprised of metamaterial inclusions

$$\psi^{\pm}(\boldsymbol{x}_\perp;\boldsymbol{q}) = E_z(\boldsymbol{x}_\perp;\boldsymbol{q}) \pm H_z(\boldsymbol{x}_\perp;\boldsymbol{q})$$

$$\left(k_0^2\mu_{zz} + \nabla_\perp \frac{1}{\epsilon_\perp}\nabla_\perp\right) H_z = \left[\nabla_\perp\left(\frac{-i\chi_{xy}}{\epsilon_\perp\,\mu_\perp}\right)\times\nabla_\perp E_z\right]_z,$$
$$\left(k_0^2\epsilon_{zz} + \nabla_\perp \frac{1}{\mu_\perp}\nabla_\perp\right) E_z = \left[\nabla_\perp\left(\frac{-i\chi_{xy}}{\epsilon_\perp\,\mu_\perp}\right)\times\nabla_\perp H_z\right]_z,$$

- By restoring polarization degeneracy $\epsilon_{zz} = \mu_{zz}$, $\epsilon_\perp = \mu_\perp$ we emulate spin degree of freedom
- Bianisotropy works as an effective spin-orbital coupling responsible for the topological transition

$$\left(k_0^2\epsilon_{zz} + \nabla_\perp \frac{1}{\mu_\perp}\nabla_\perp\right)\psi^{\pm} = \pm\left[\nabla_\perp\left(\frac{-i\chi_{xy}}{\epsilon_\perp\,\mu_\perp}\right)\times\nabla_\perp\psi^{\pm}\right]_z$$

$$T\,\psi^{\pm}(\boldsymbol{x}_\perp;\boldsymbol{q}) = \psi^{\mp}(\boldsymbol{x}_\perp;-\boldsymbol{q})$$

Khanikaev *et al.*, Photonic Topological Insulators, Nat. Mater. **12**, 233 (2012).

Photonic Topological Insulators: QSHE

$l = \pm 1$ (dipolar) degeneracy

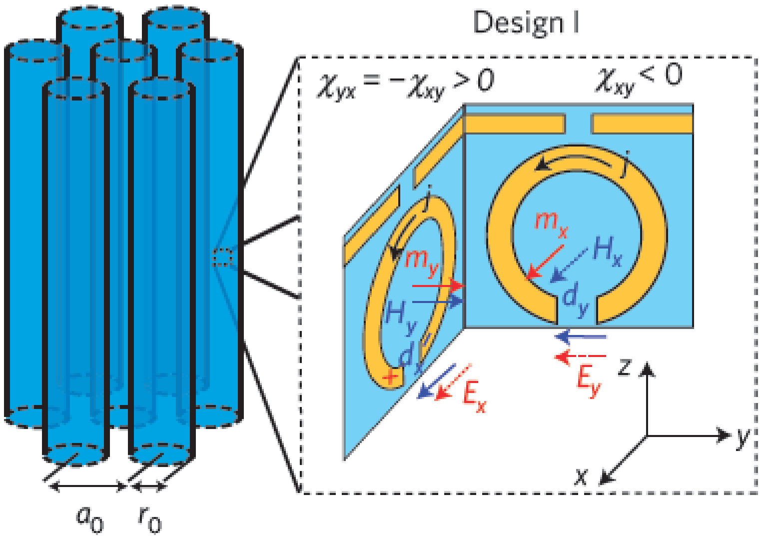

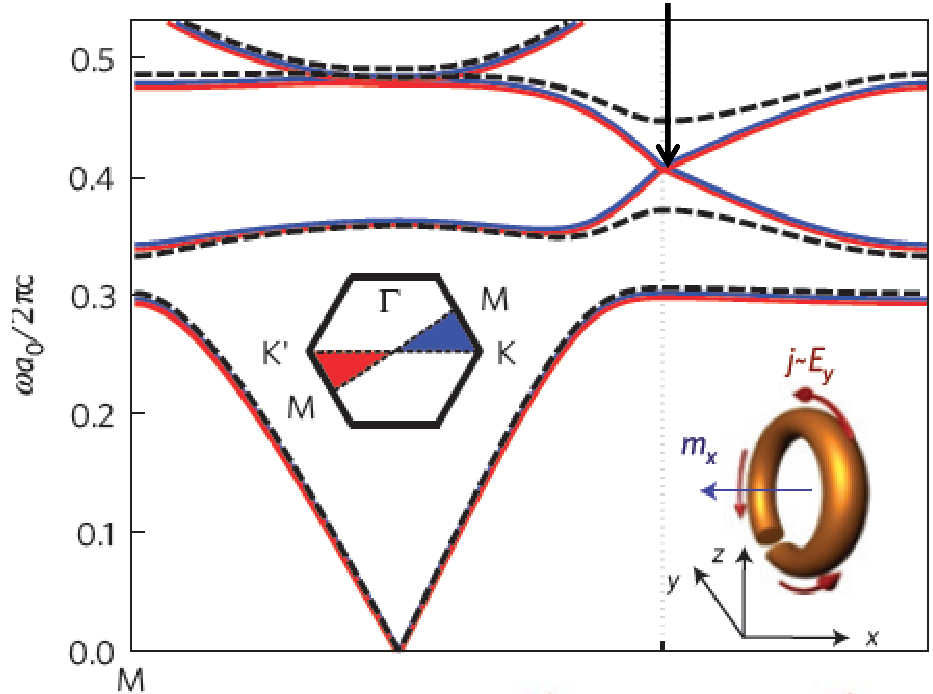

Nothing new… unless the bianisotropy is **ON**

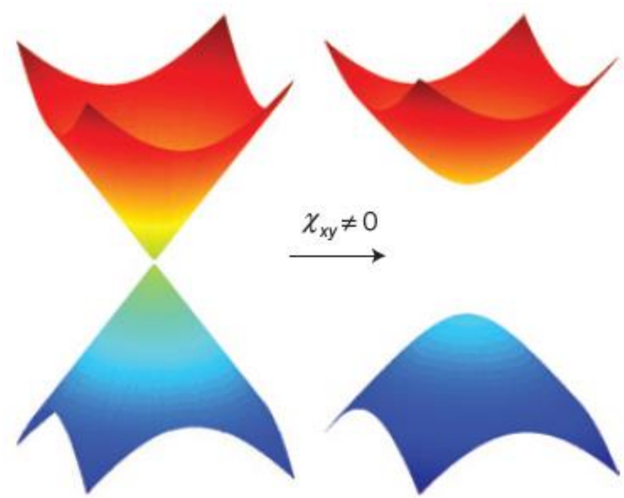

•Without bianisotropy (no gap): photonic crystal with double Dirac point

•With bi-anisotropy (gapped PBS): photonic QSHE insulator

Topological invariants of the photonic topological insulator

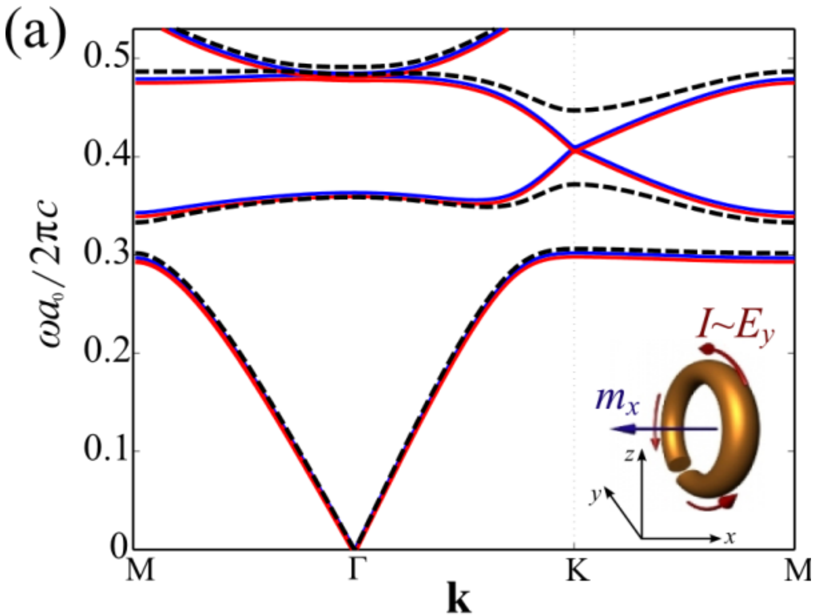

$$A_n^{\pm} = -i\langle \boldsymbol{\psi}^{n\pm}(\mathbf{k})|\nabla_{\mathbf{k}}|\boldsymbol{\psi}^{n\pm}(\mathbf{k})\rangle$$

$$C_n^{\pm} = \pm\frac{1}{2\pi}\int_{\mathrm{BZ}} d^2\boldsymbol{k}\left[\partial_{k_x}A_y^{n\pm}(\boldsymbol{k}) - \partial_{k_y}A_x^{n\pm}(\boldsymbol{k})\right]$$

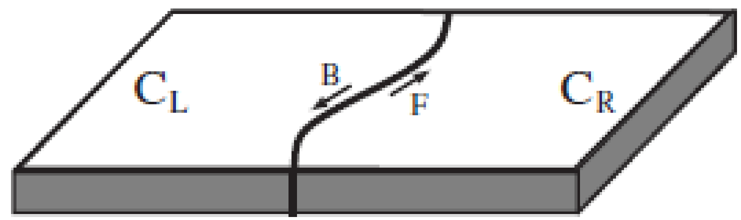

$\boldsymbol{\psi}^{+} = \boldsymbol{E}_z + \boldsymbol{H}_z$

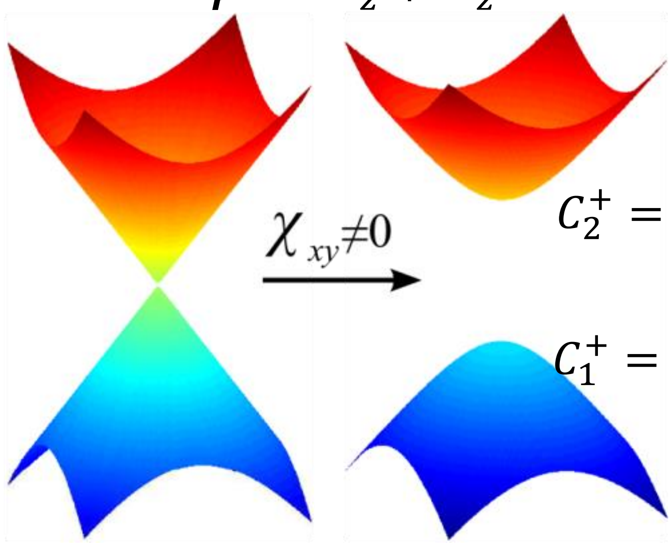

$C_2^{+} = -1$

$C_1^{+} = 1$

$\boldsymbol{\psi}^{-} = \boldsymbol{E}_z - \boldsymbol{H}_z$

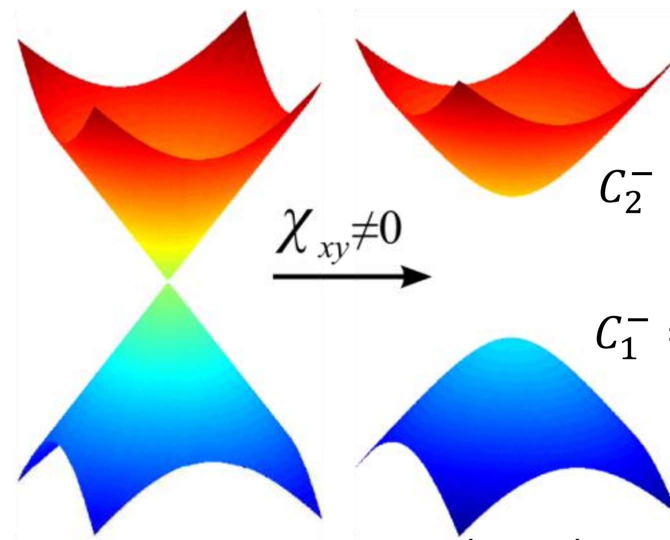

$C_2^{-} = 1$

$C_1^{-} = -1$

Khanikaev *et al.*, Photonic Topological Insulators, Nat. Mater. **12**, 233 (2012).

Spin-Polarized Surface (edge) States

Matching gaps of trivial and nontrivial insulators to avoid leaks

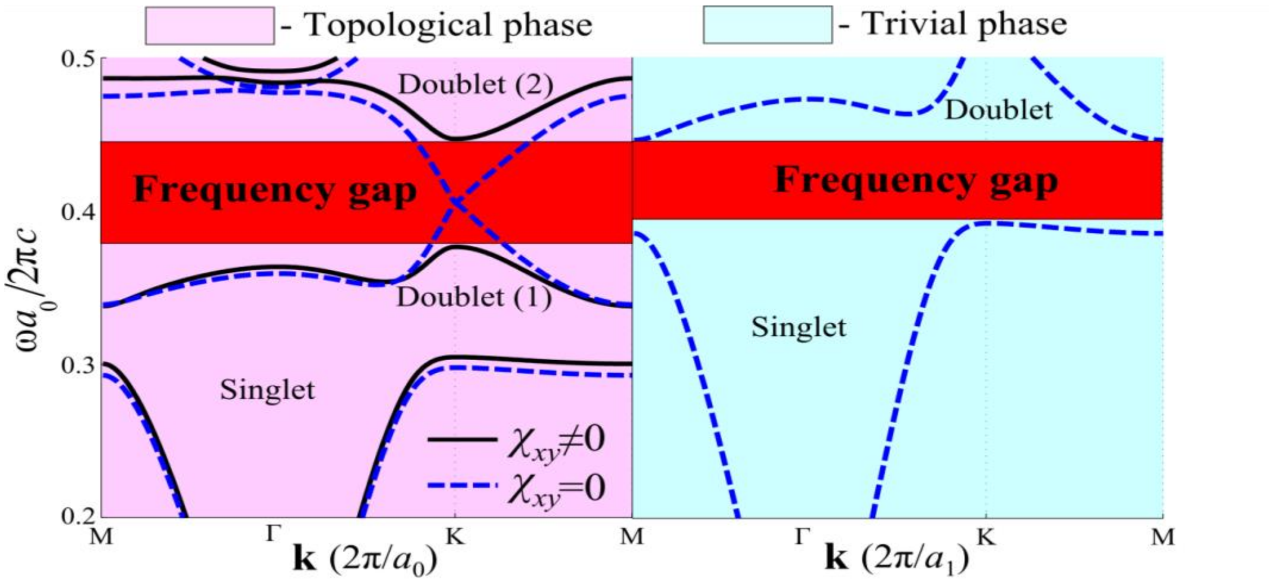

Selective excitation of spin-up and spin-down edge states

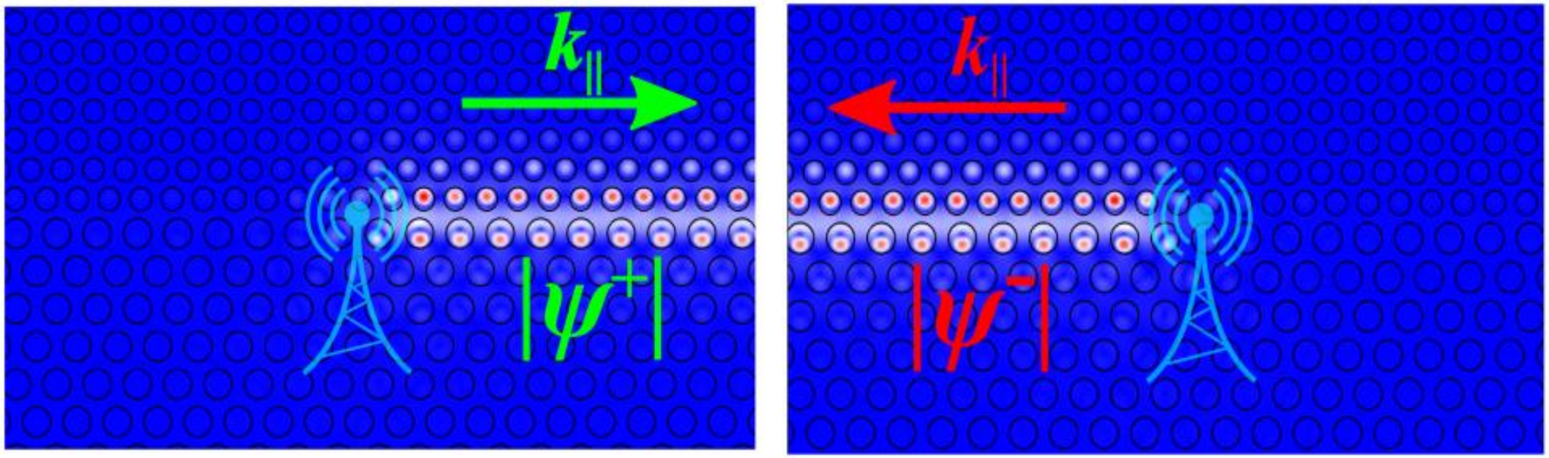

Topological protection of spin-locked edge states

(i) Robustness against scattering by sharp bends

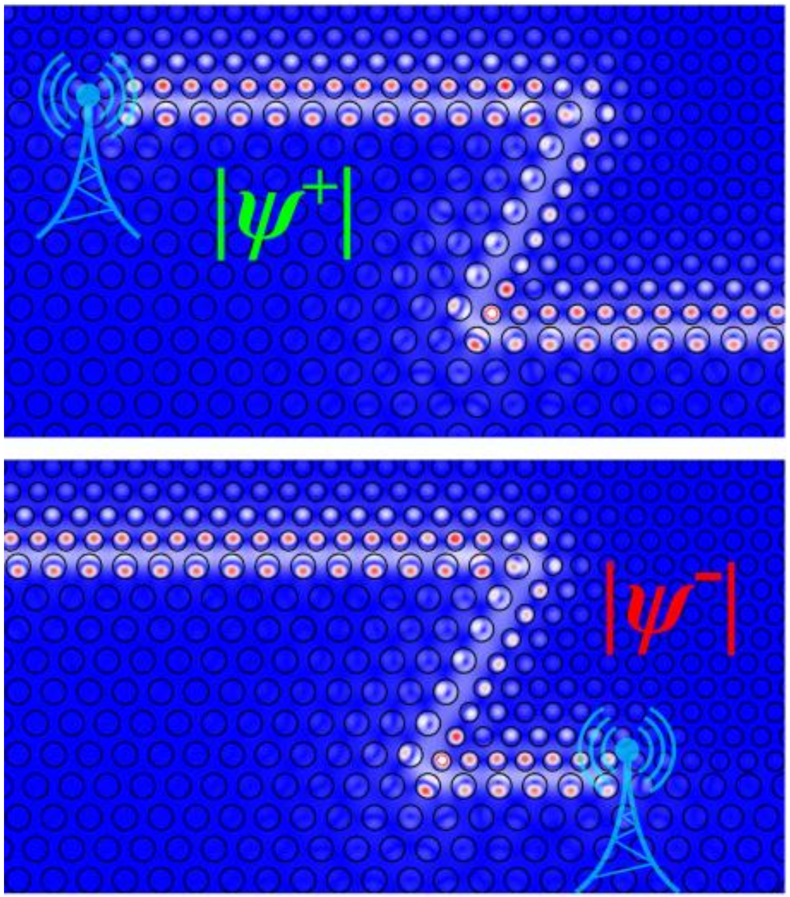

(ii) Tunneling through the cavity at any frequency within the gap (not only at Fabry-Perot resonances)

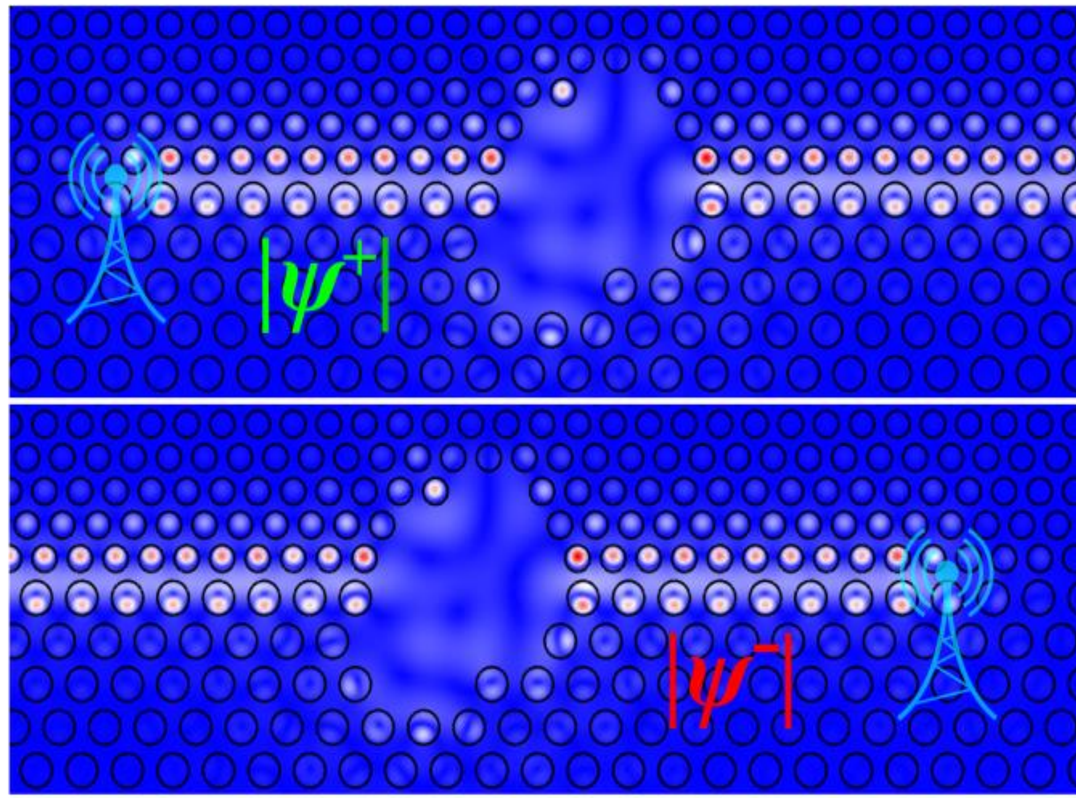

Khanikaev *et al.*, Photonic Topological Insulators, Nat. Mater. **12**, 233 (2012).

Practical designs of photonic topological insulators

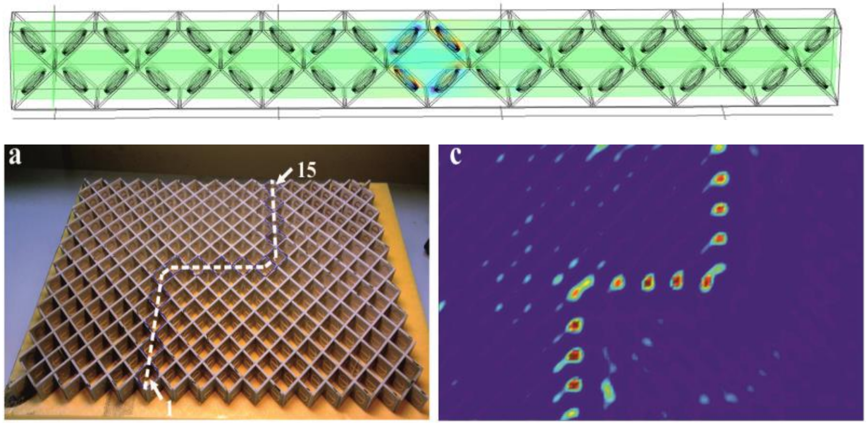

A. P. Slobozhanyuk, et al., arXiv:1507.05158 (2015)
Scientific Reports **6**, 22270 (2016).

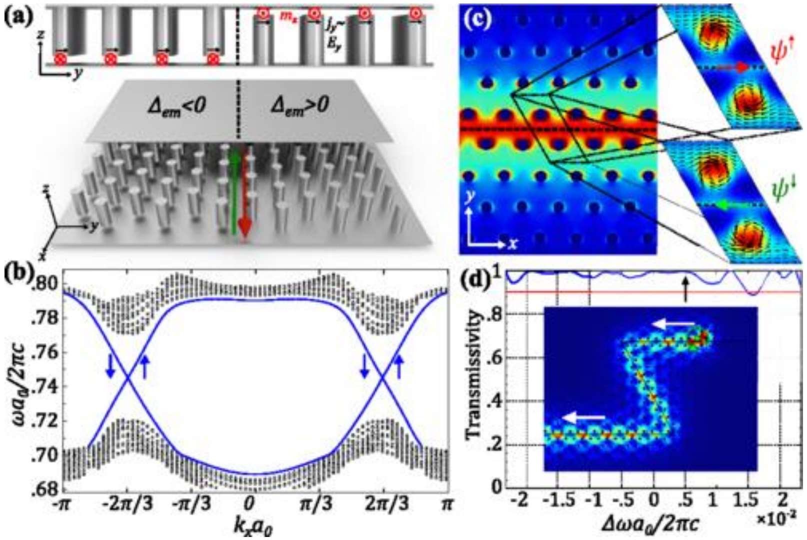

T. Ma et al., arXiv:1401.1276 (2014), Phys. Rev. Lett. **114**, 127401 (2015).

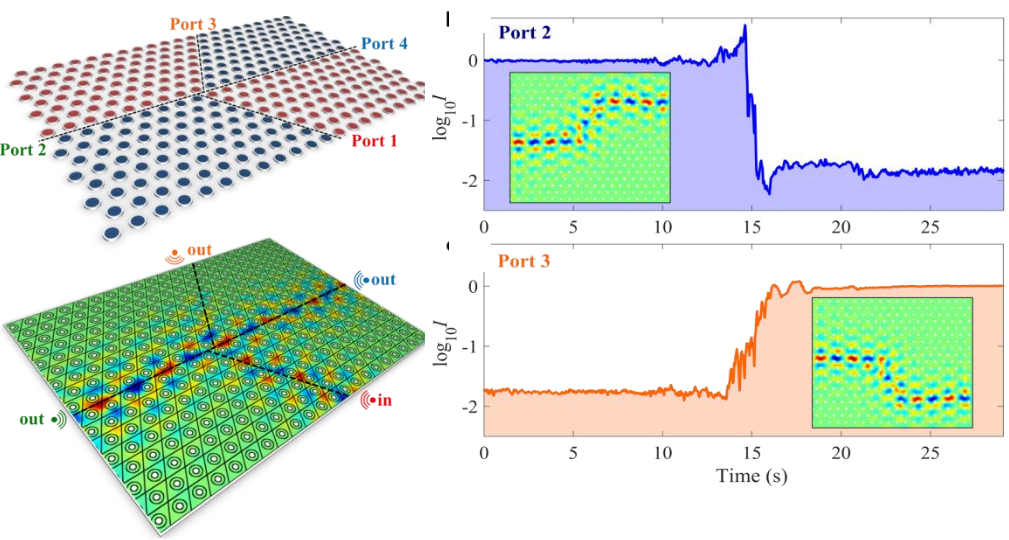

X. Cheng et al., Nature Materials **15**, 542–548 (2016).

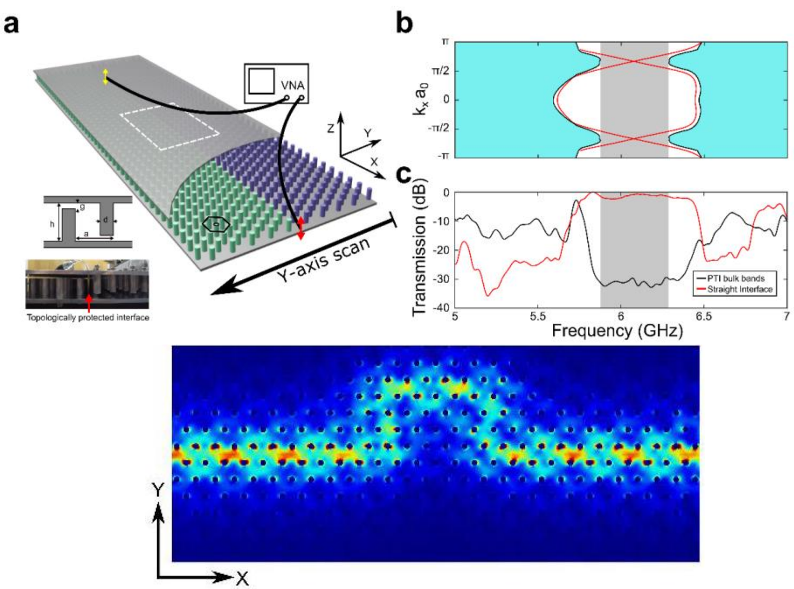

K. Lai et al., arXiv:1601.01311v2 (2016).

Reconfigurable photonic topological insulator

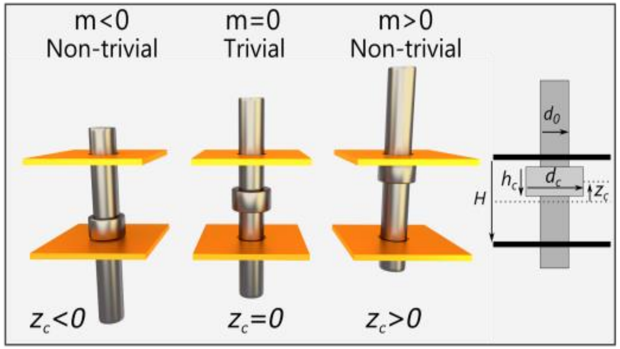

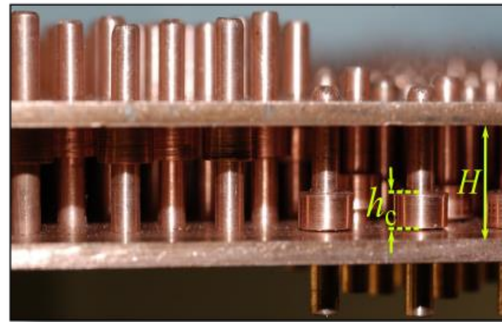

without top plate

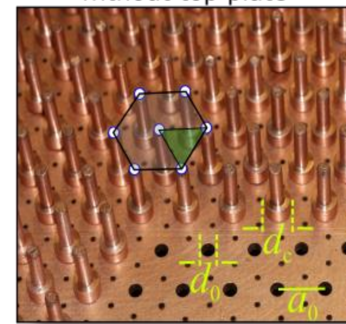

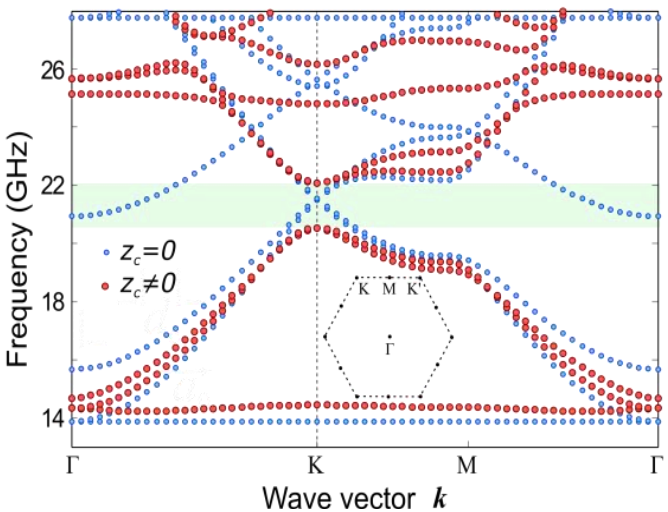

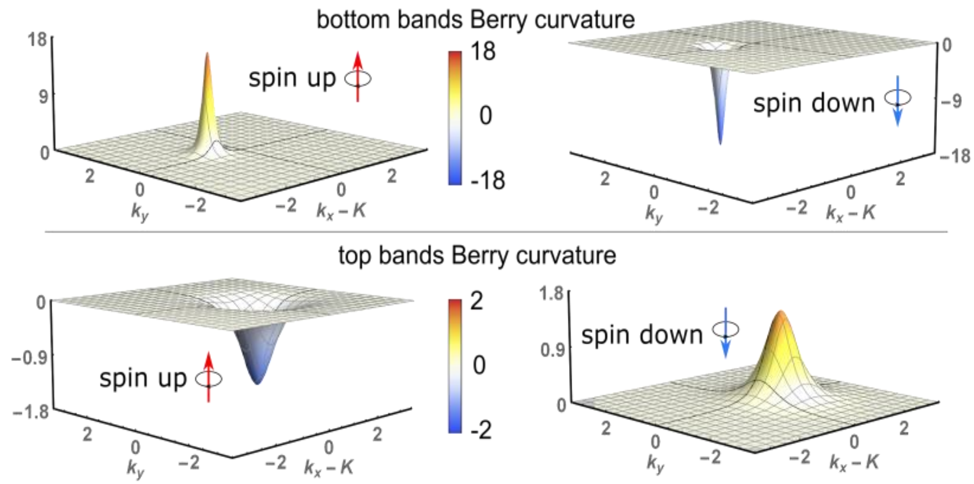

Effective Kane-Mele-like Hamiltonian

$$\hat{\mathcal{H}}_{\uparrow/\downarrow} = v_D \hat{\tau}_0 \hat{s}_0 \hat{\boldsymbol{\sigma}}_\parallel \cdot \delta \boldsymbol{k}_\parallel + m \hat{\tau}_3 \hat{s}_3 \hat{\sigma}_3$$

Non-vanishing spin-Chern numbers

$$C^{\uparrow}_{u/l} = \pm \frac{m}{|m|} \text{ and } C^{\downarrow}_{u/l} = \mp \frac{m}{|m|}$$

X. Cheng, C. Jouvaud, X. Ni, S. H. Mousavi, A. Z. Genack, and **A. B. Khanikaev**, *Robust propagation along reconfigurable pathways within a photonic topological insulator*, Nature Materials **15**, 542–548 (2016).

Topological edge states

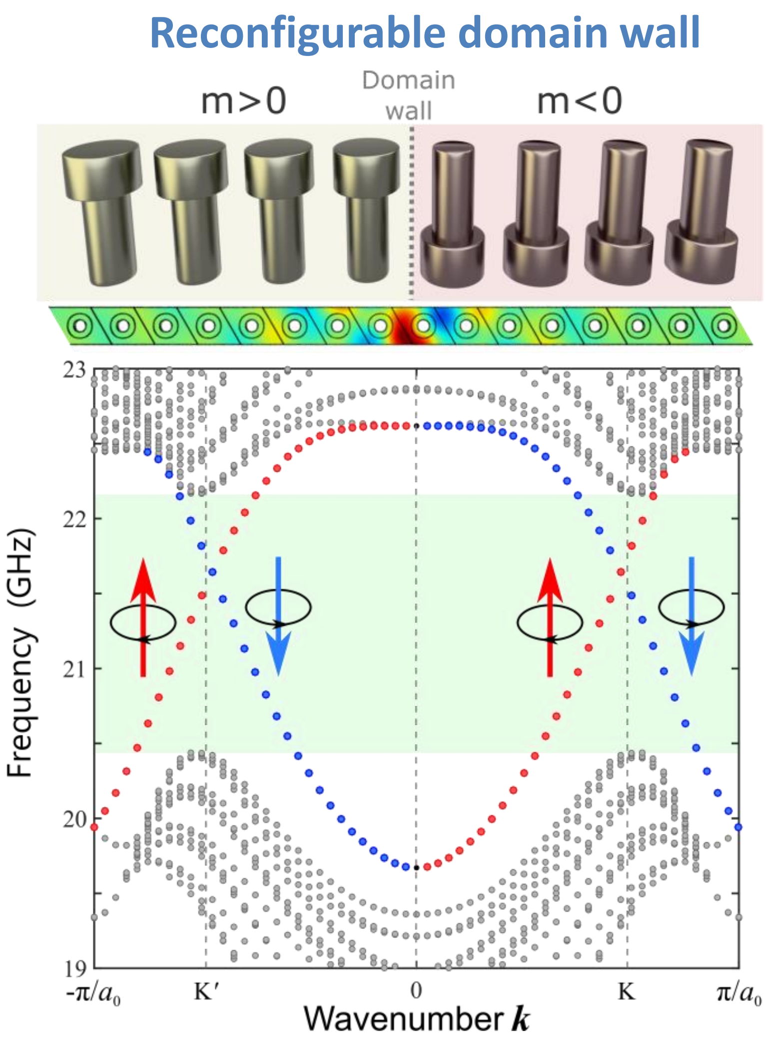

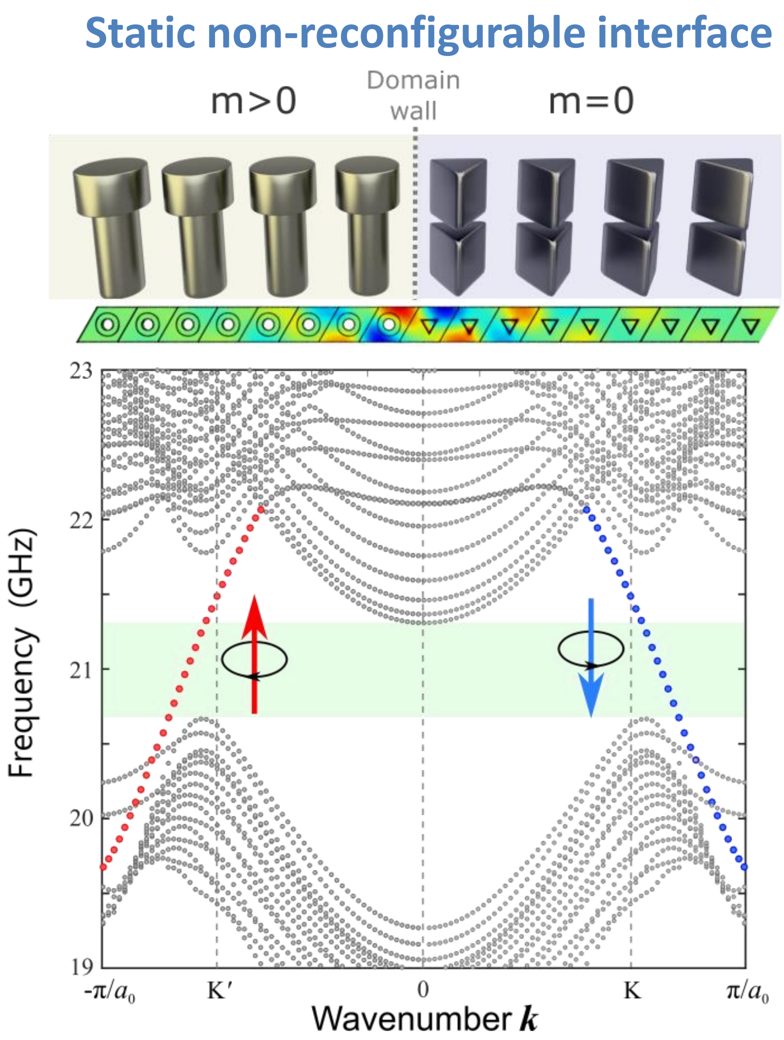

Nature Materials **15**, 542–548 (2016).

Reconfigurable guiding along arbitrarily shaped pathways

Two 60 deg. bends

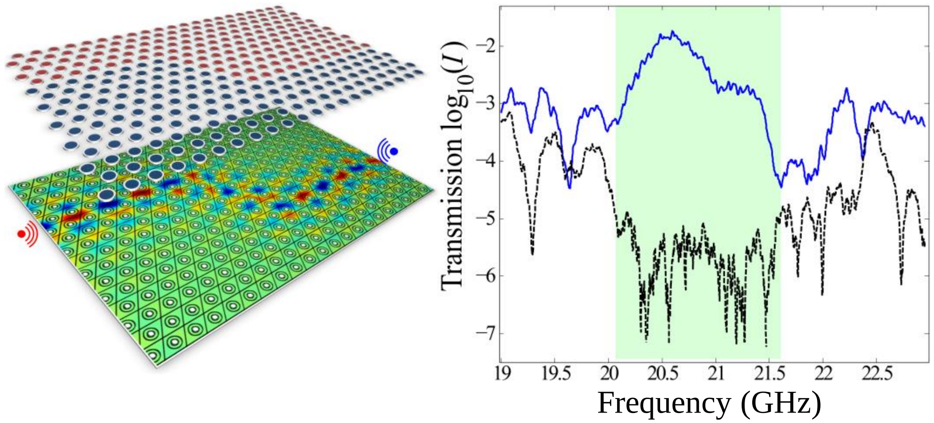

Two 90 deg. bends

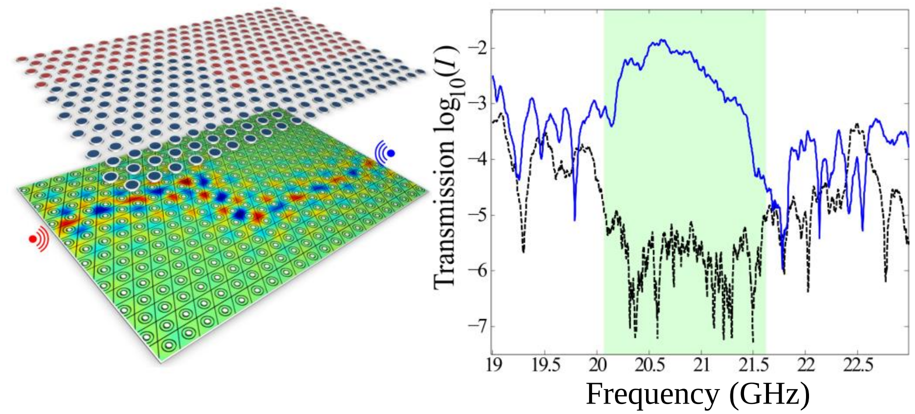

Two 120 deg. bends

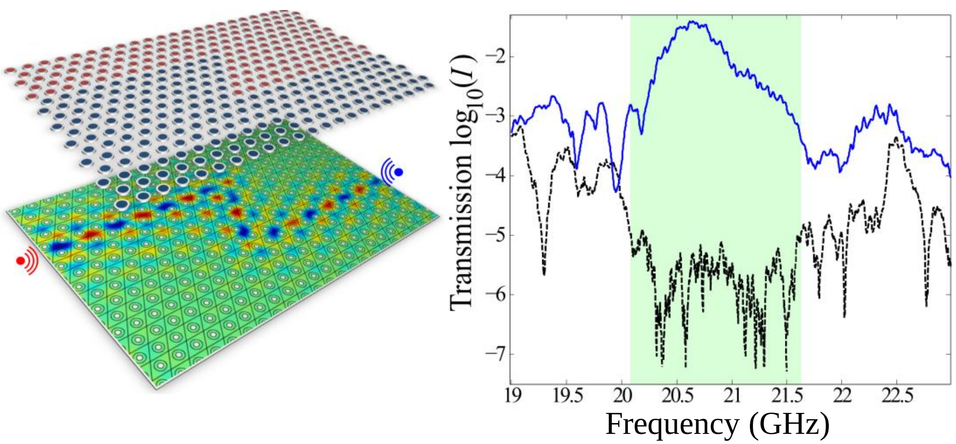

---------- Transmission through the bulk

—— Transmission through the domain wall

Exponential localization of the edge states

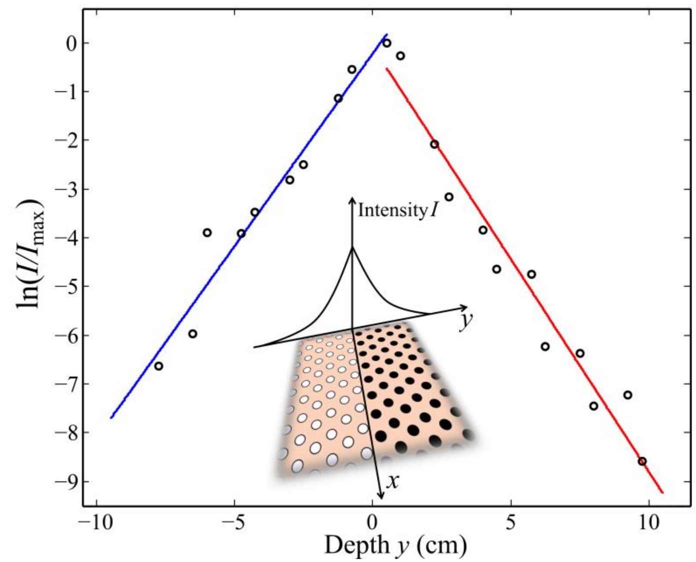

Nature Materials **15**, 542–548 (2016).

Robustness against disorder

Experimental demonstration of ballistic transport of the topological edge modes through randomly shaped domain walls and disordered regions

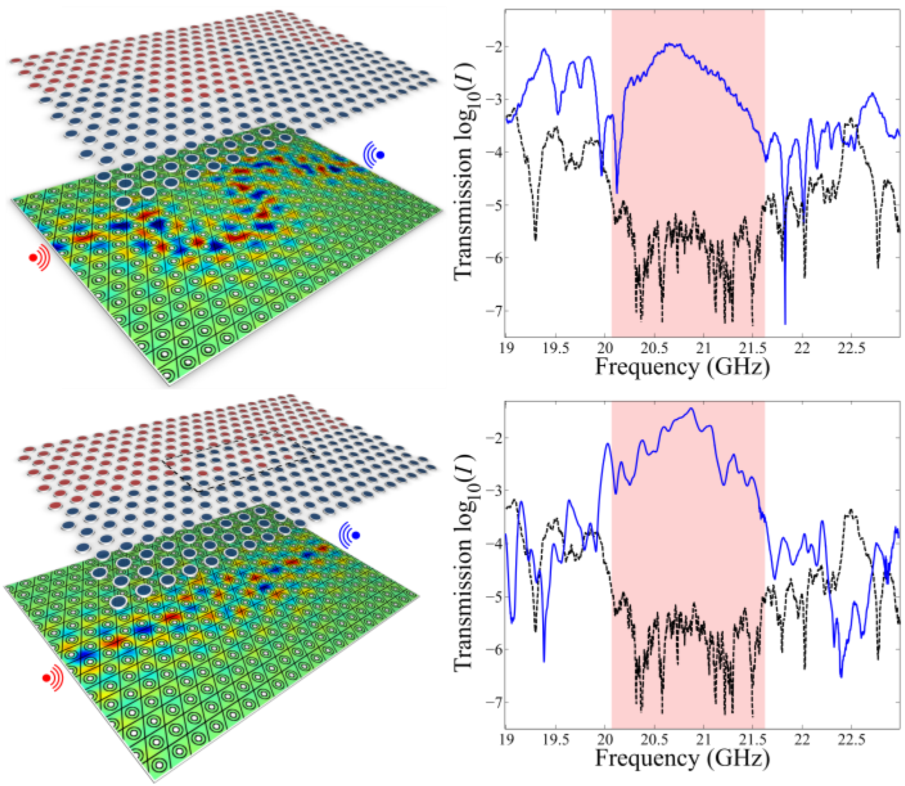

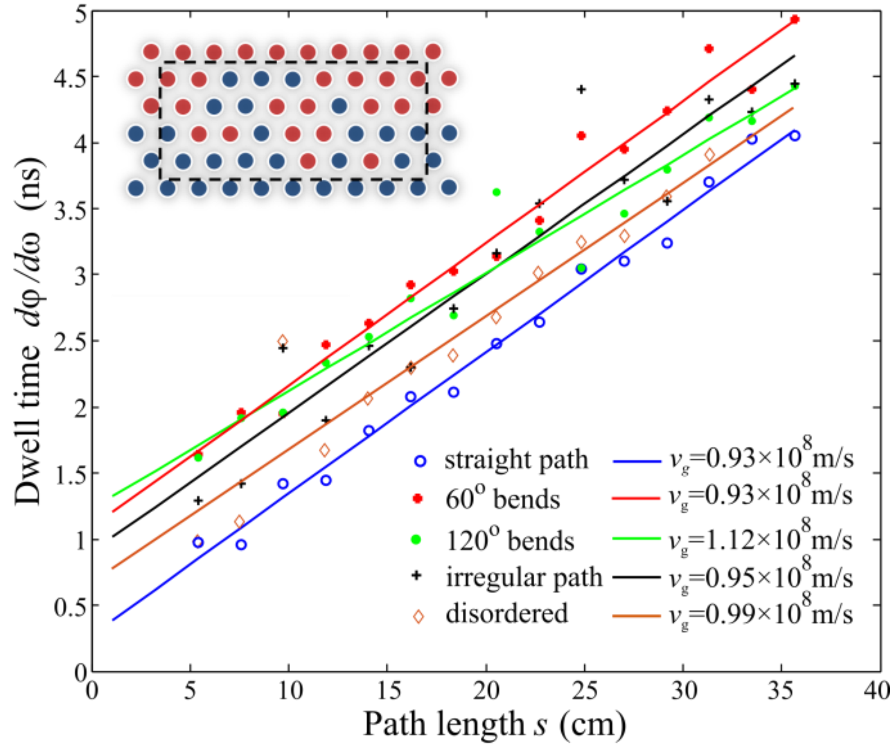

X. Cheng, C. Jouvaud, X. Ni, S. H. Mousavi, A. Z. Genack, and A. B. Khanikaev, *Robust propagation along reconfigurable pathways within a photonic topological insulator*, Nature Materials **15**, 542–548 (2016).

Demonstration of spin-locking of the topological edge states

Experimental proof of spin-locked wave-division of an edge mode at a four-port topological junction.

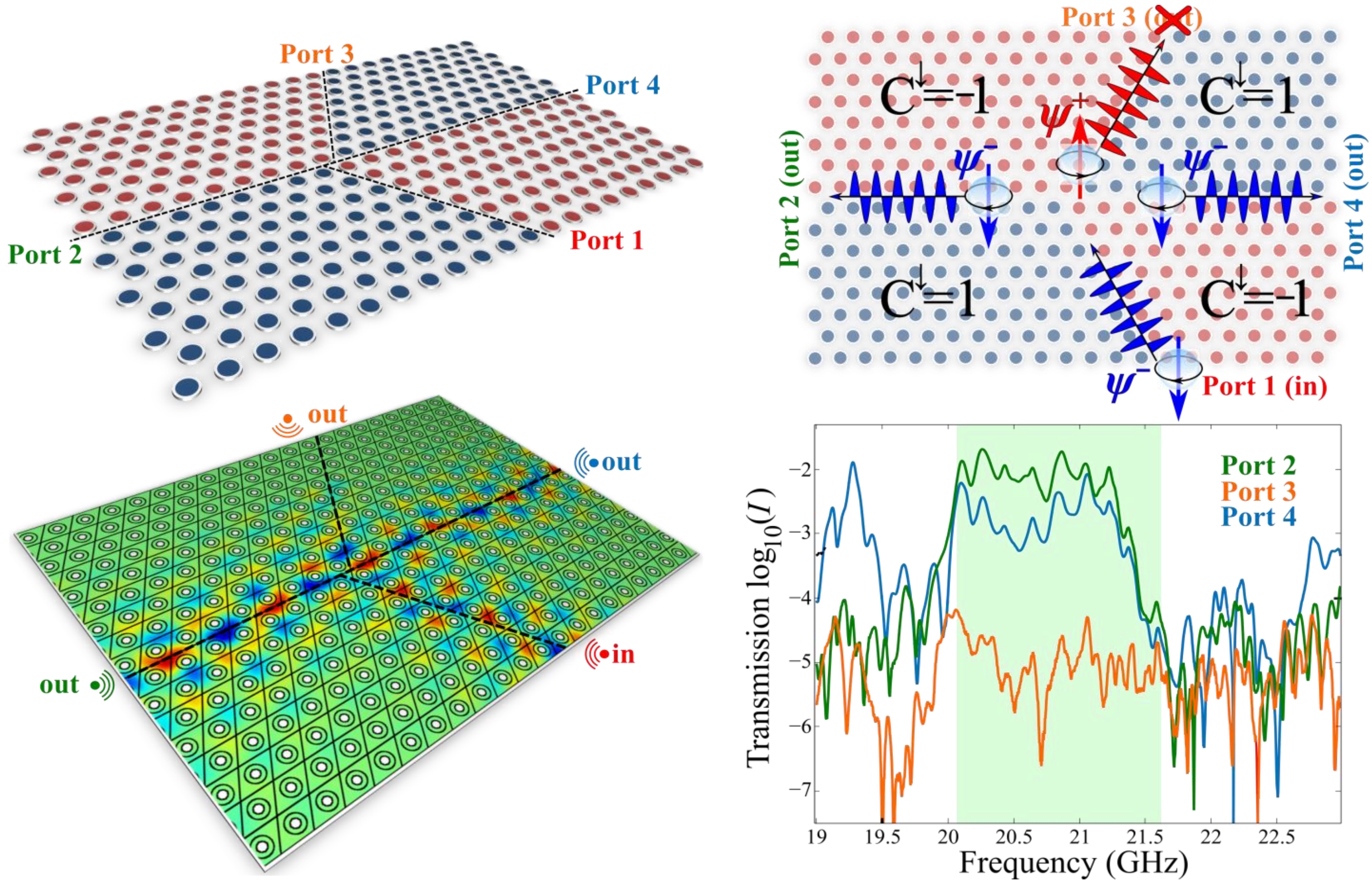

Nature Materials **15**, 542–548 (2016).

Motivation to move to “all-dielectric” and 3D

i) Moving to optical domain
ii) Rich 3D physics: Weyl points and “true” Dirac points
iii) Avoiding magnetic materials:
symmetry-protected topological order without breaking TR

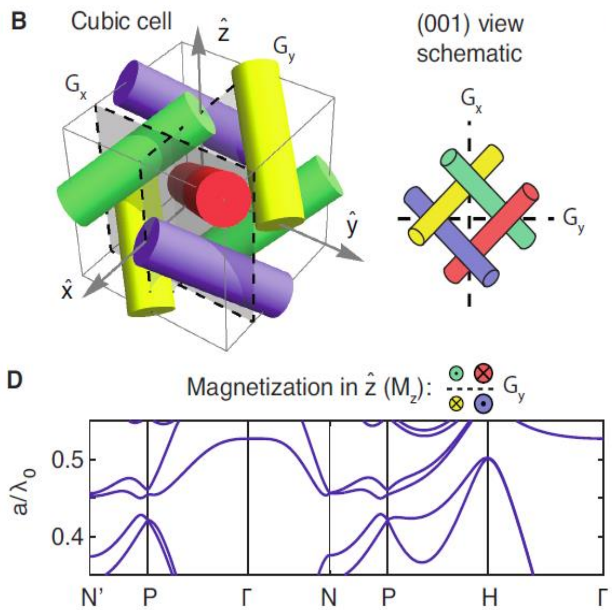

Soljačić group: Symmetry-protected topological photonic crystal in three dimensions, Ling Lu et al., Nature Physics 12, 337–340 (2016).

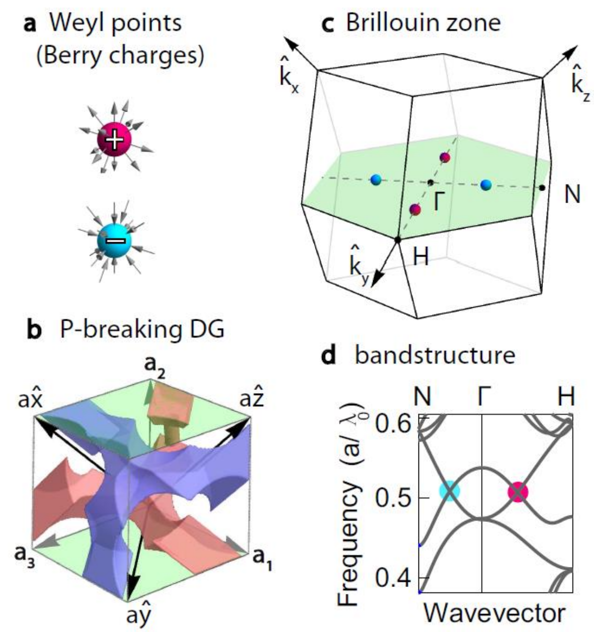

A. Slobozhanyuk, S. H. Mousavi, X. Ni, D. Smirnova, Y. S. Kivshar, & A. B. Khanikaev, Nature Photonics **11**, 130-136 (2017) ,doi:10.1038/nphoton.2016.253

2D all-dielectric photonic topological metasurface

Degeneracy between magnetic and electric dipolar modes of the cylinders + all-dielectric bianisotropy

Even (+): + + Electric dipolar

Odd (-): + – Magnetic dipolar

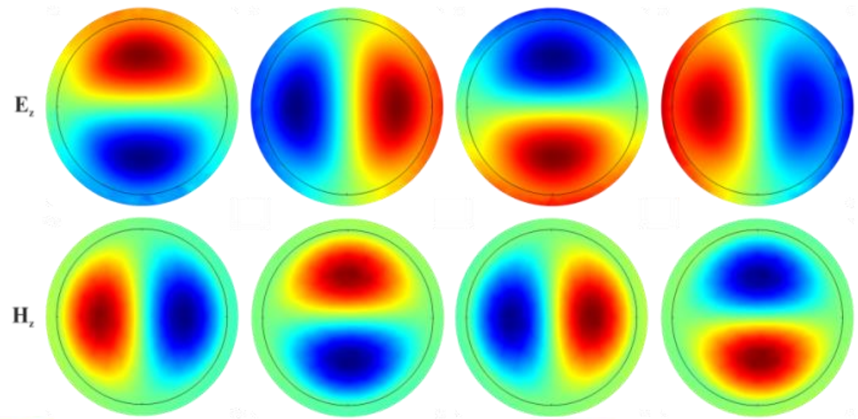

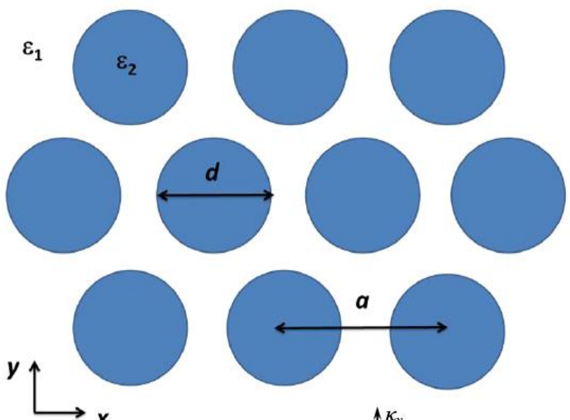

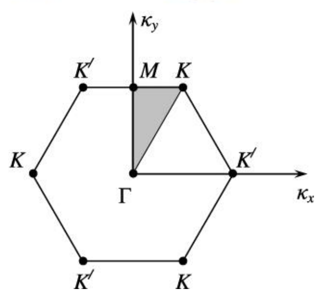

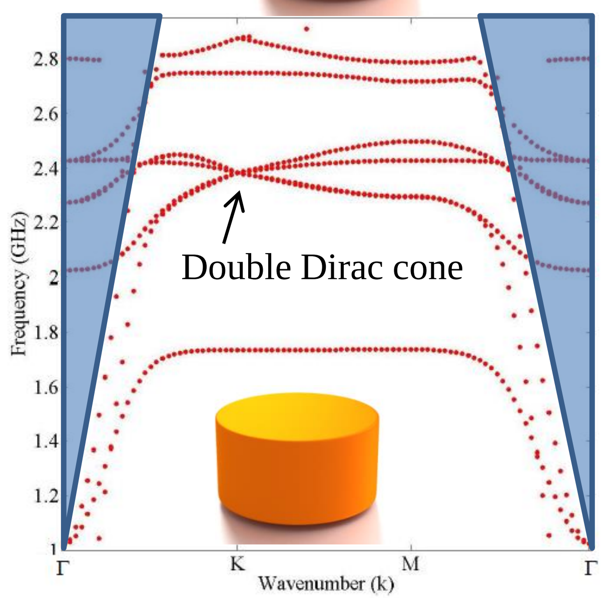

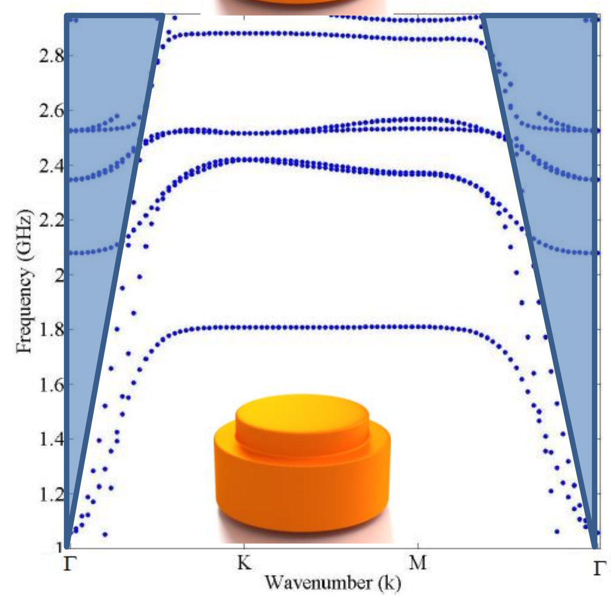

2D all-dielectric photonic topological metasurface

Reversal of bianisotropy to create topological domain walls

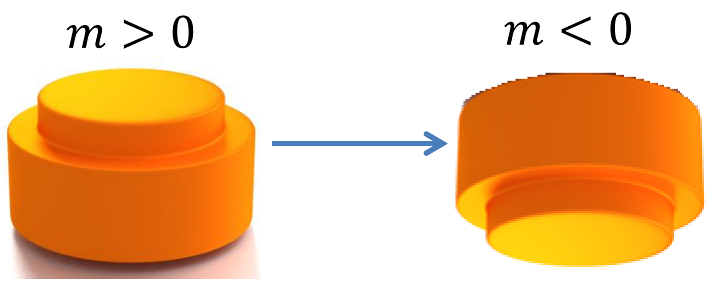

$$\widehat{\mathcal{H}}_{\uparrow/\downarrow} = v_D \hat{\tau}_0 \hat{s}_0 \widehat{\boldsymbol{\sigma}}_\parallel \cdot \delta \boldsymbol{k}_\parallel + m \hat{\tau}_3 \hat{s}_3 \hat{\sigma}_3$$

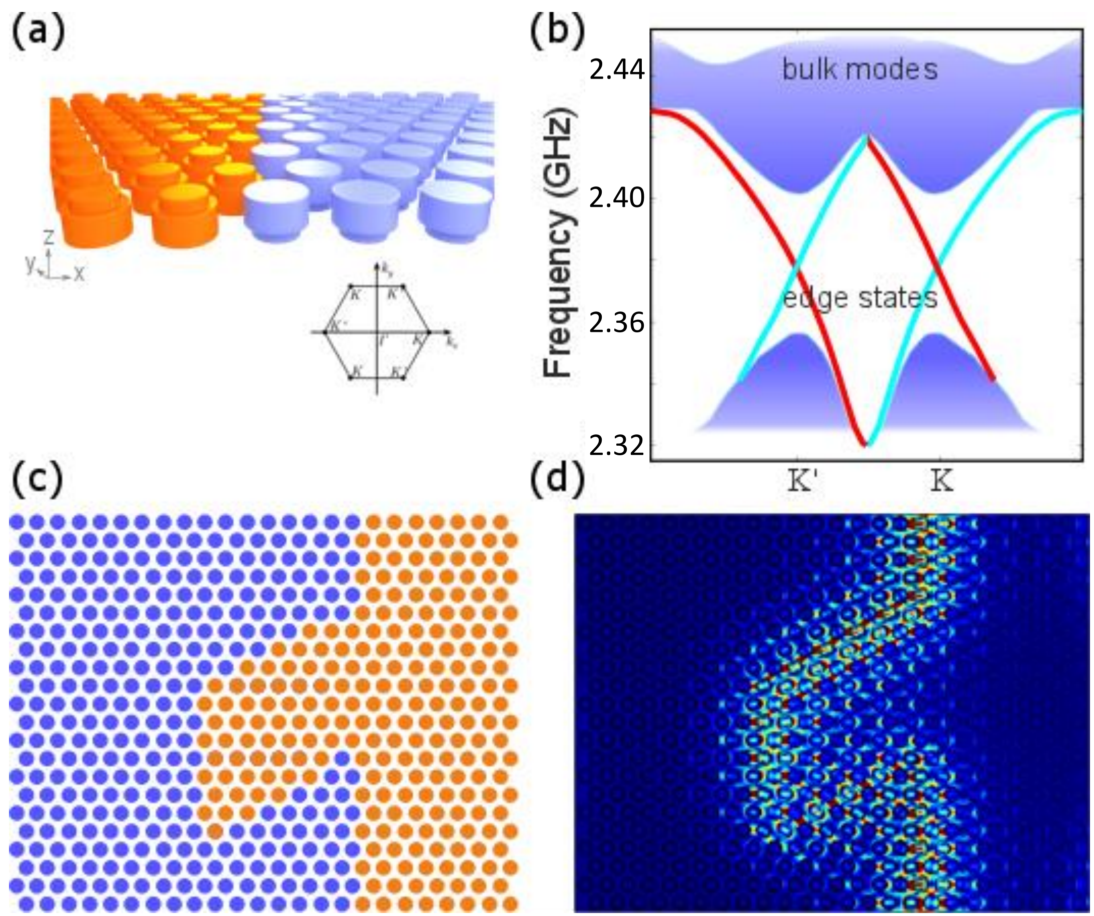

Experimental realization

Experiment: spin-locking

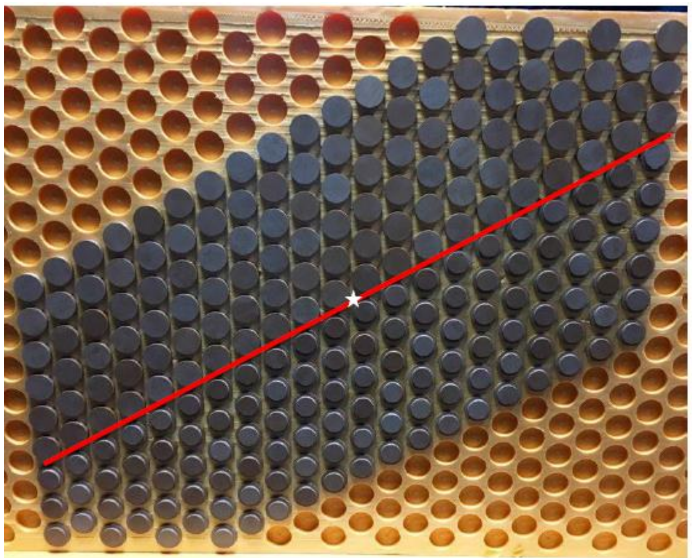

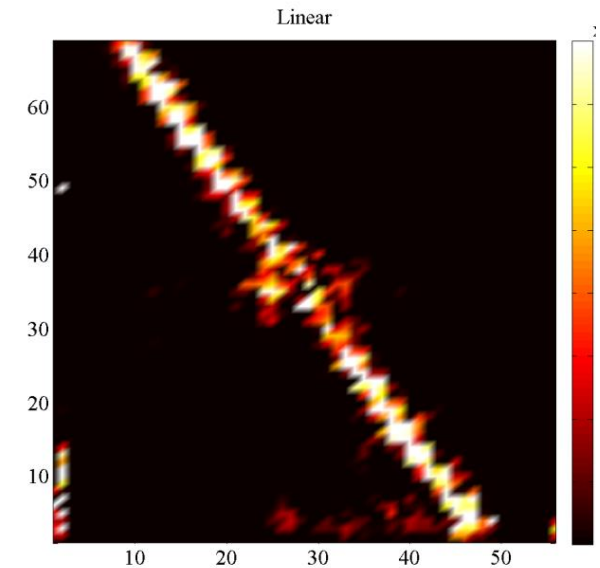

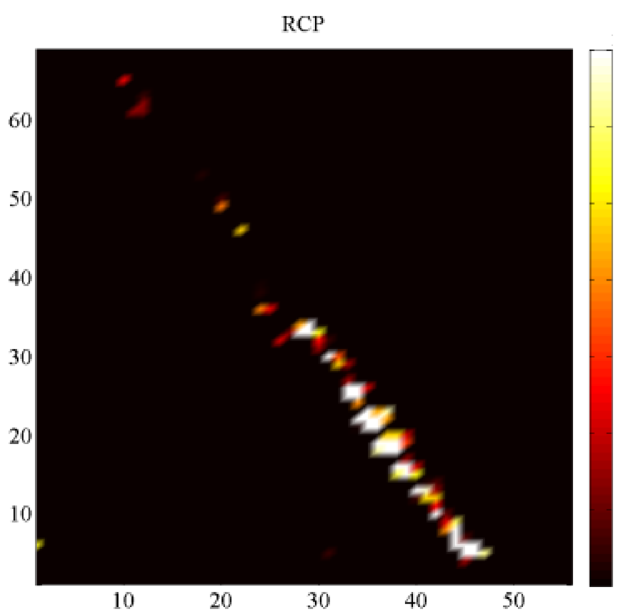

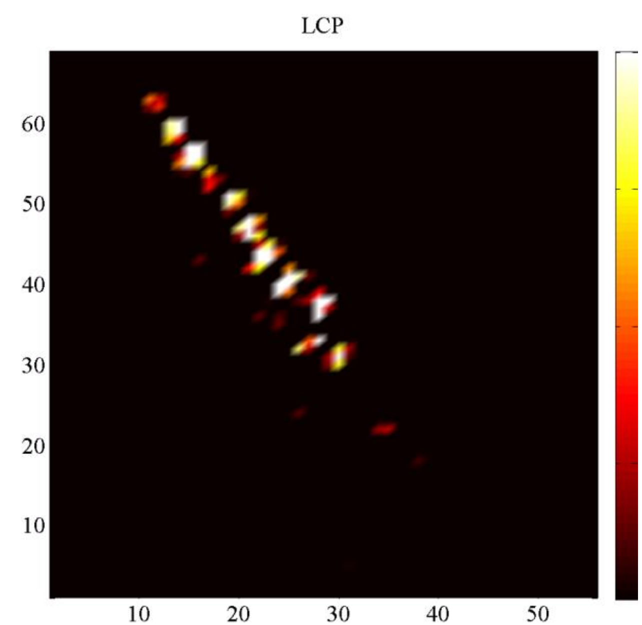

Experiment: sharp bends

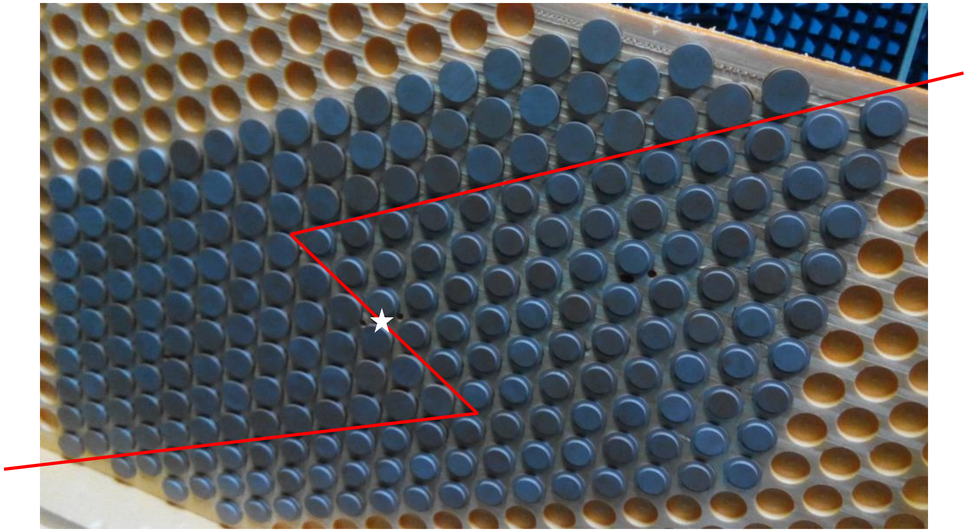

LINEAR

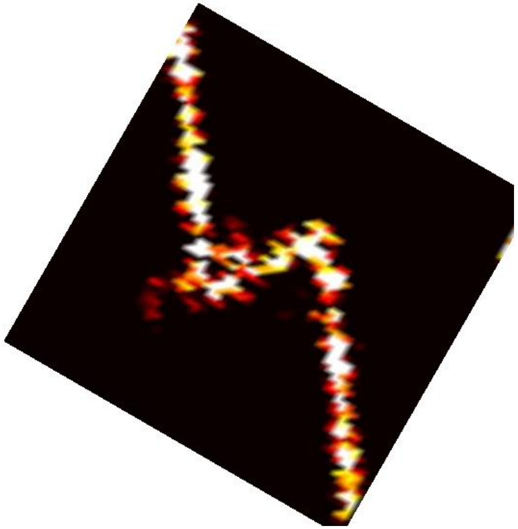

RCP

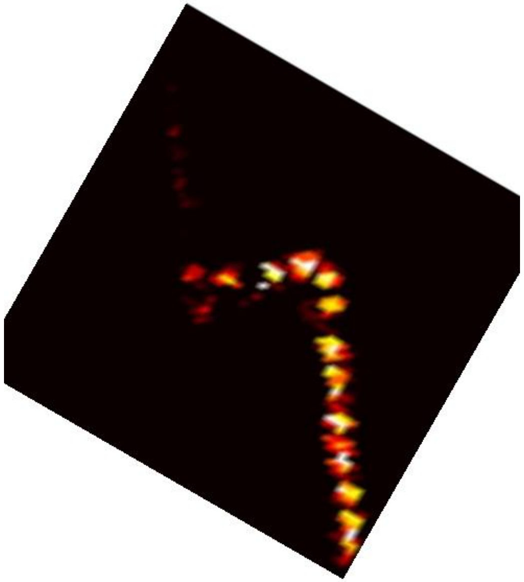

LCP

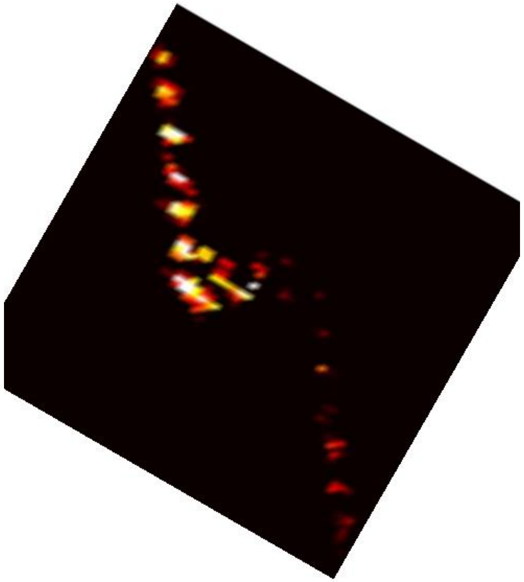

3D Photonic dual-symmetric metacrystal

Weak topological insulator – stacking of 2D TIs

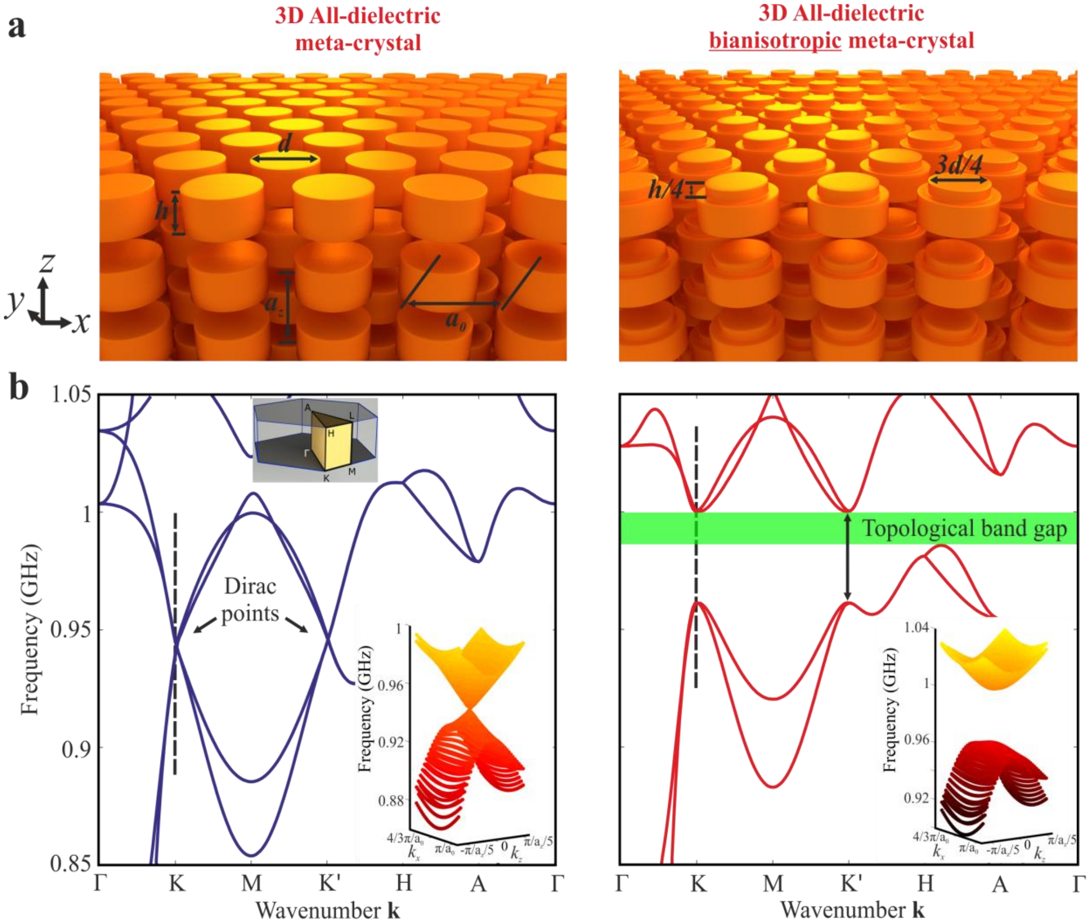

Degeneracy between magnetic and electric dipolar modes of the cylinders + all-dielectric bianisotropy

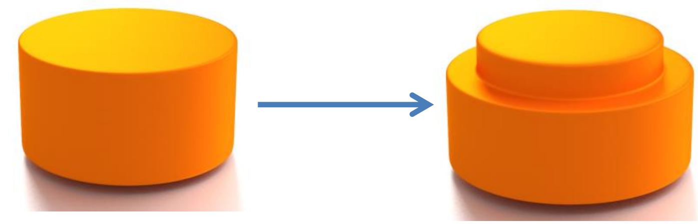

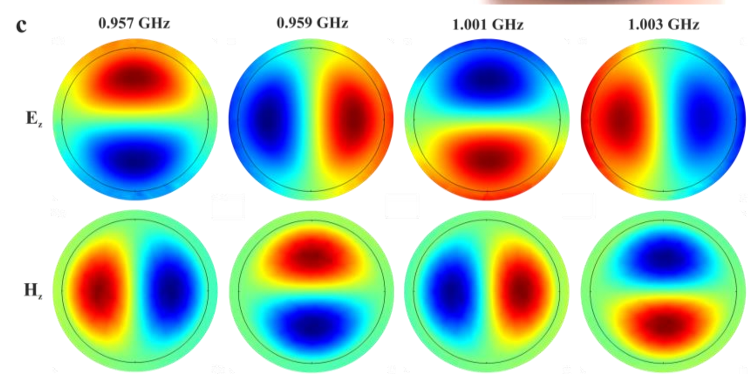

$$\widehat{\mathcal{H}} = \omega_0 + v_{||}\hat{s}_0\left(\delta k_x\hat{\sigma}_x + \delta k_y\hat{\sigma}_y\right) + v_z\hat{s}_y\hat{\sigma}_z\delta k_z + m\hat{s}_z\hat{\sigma}_z$$

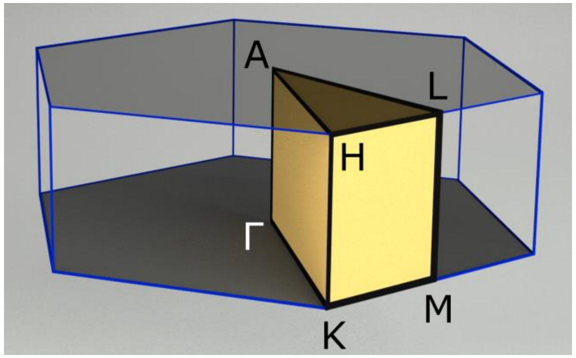

Nature Photonics (2017) ,doi:10.1038/nphoton.2016.253

Electromagnetic perturbation theory

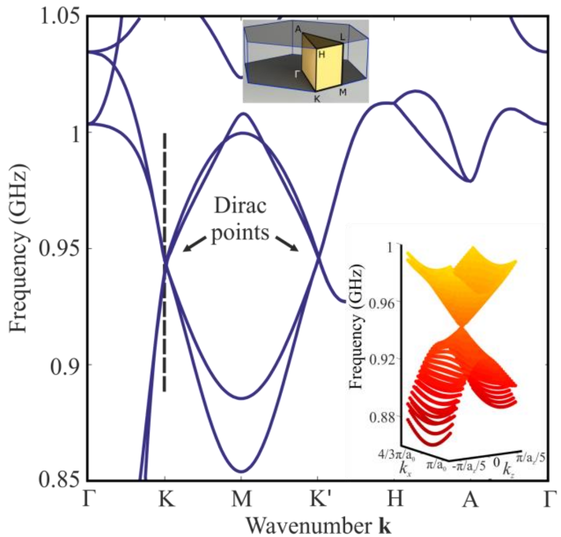

$$\hat{\mathcal{H}}_K = \omega_0 \hat{s}_0 \hat{\sigma}_0$$

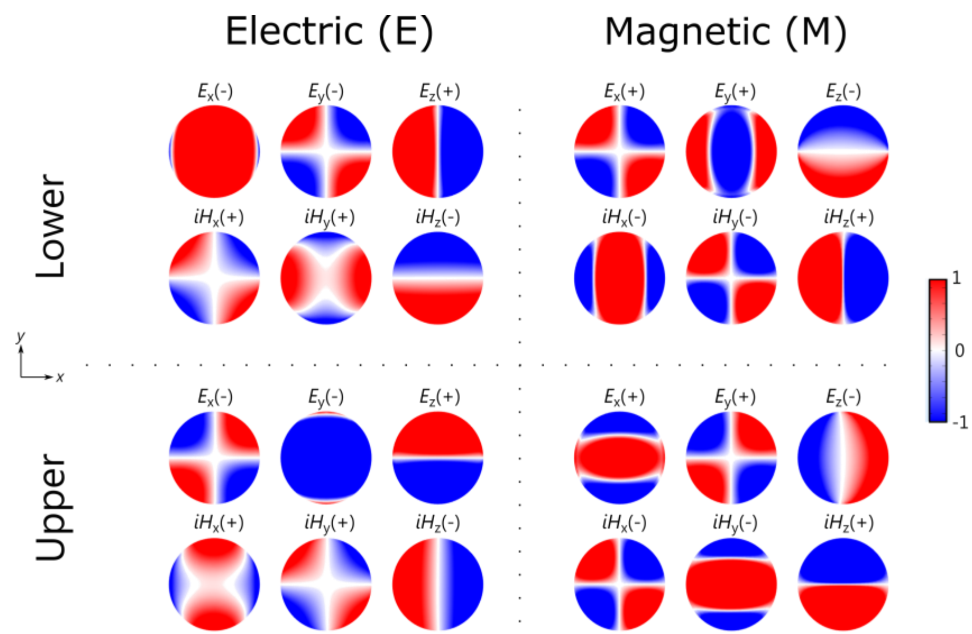

Two mechanisms of bianisotropy:

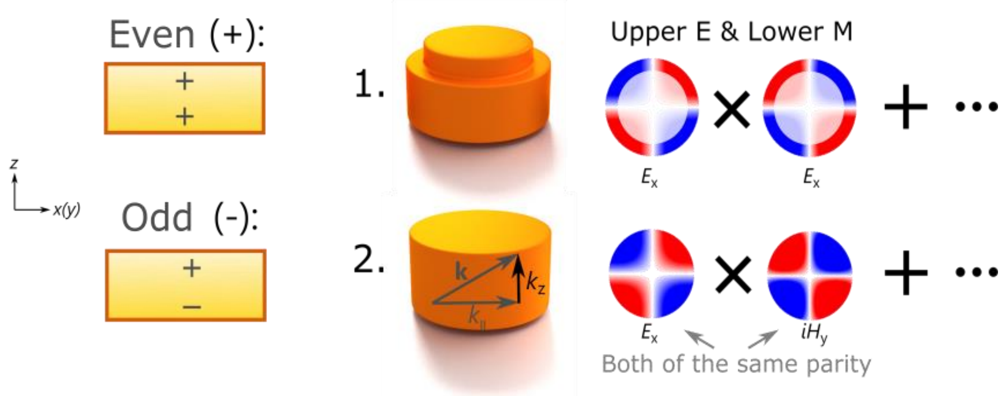

Dielectric perturbation

$$\Delta_{mn} = -\int d^3r\, \delta\epsilon_r\, \epsilon_0 \mathbf{E}_n \cdot \mathbf{E}_m^*$$

k.p perturbation

$$\{S_i\}_{mn} = \int_V d^3r\ \{\mathbf{E}_n^* \times \mathbf{H}_m + \mathbf{E}_m \times \mathbf{H}_n^*\}_i$$

$$\hat{\mathcal{H}} = \omega_0 \hat{s}_0 \hat{\sigma}_0 + v_{||} \hat{s}_0 (\delta k_x \hat{\sigma}_x + \delta k_y \hat{\sigma}_y) + v_z \hat{s}_y \hat{\sigma}_z \delta k_z + m \hat{s}_z \hat{\sigma}_z$$

3D Dirac Hamiltonian!

Topological edge states of 2D domain walls

$$\hat{\mathcal{H}} = \omega_0 + v_{||}\hat{s}_0\left(\delta k_x\hat{\sigma}_x + \delta k_y\hat{\sigma}_y\right) + v_z\hat{s}_y\hat{\sigma}_z\delta k_z \pm m\hat{s}_z\hat{\sigma}_z$$

Jackiw-Rebbi-like surface states: $\Omega_\pm = \pm\sqrt{\zeta^2 + v_F^2\left(k_x^2 + k_y^2\right) + v_z^2 k_z^2}$

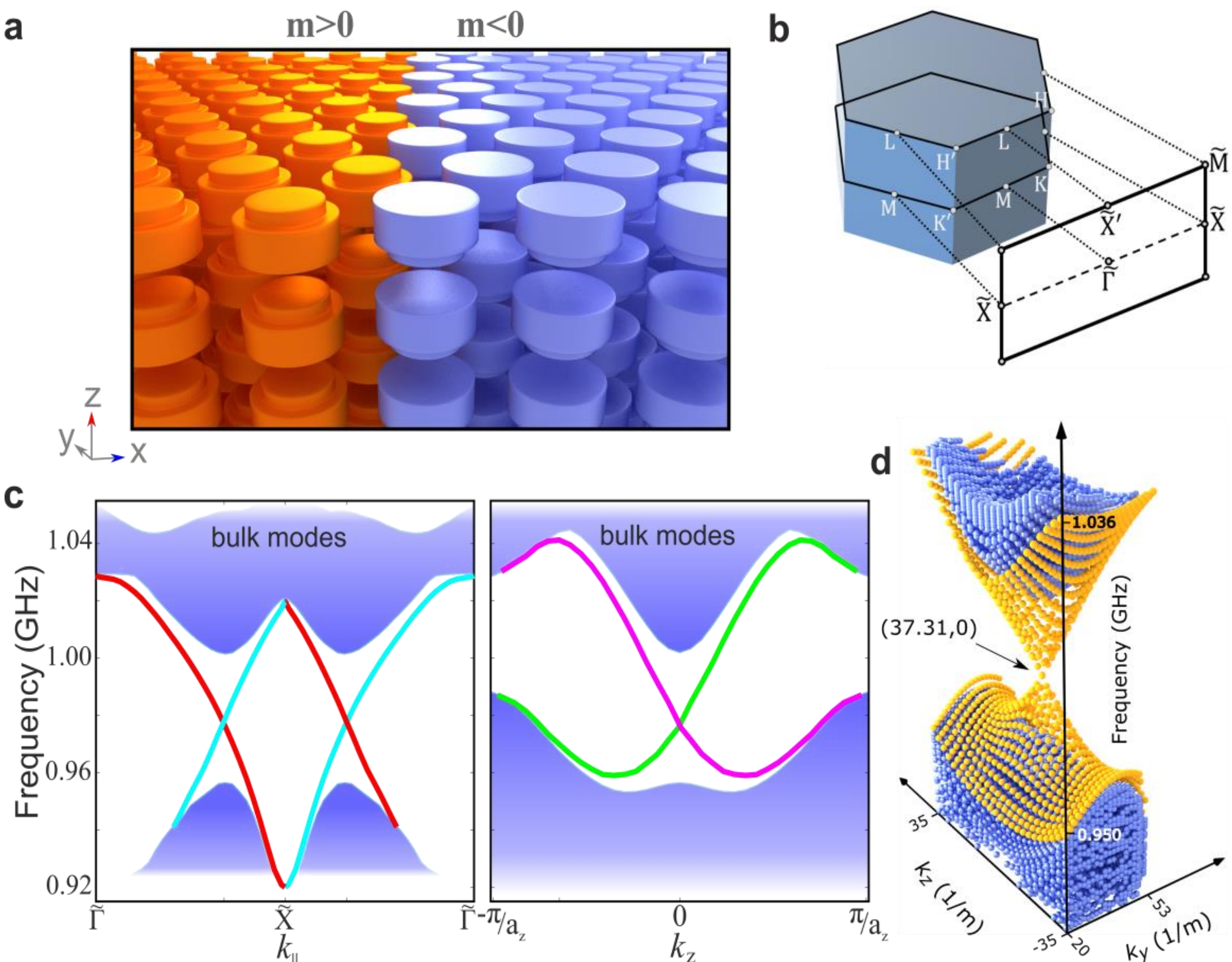

Spin-locking of edge states on 2D domain walls

$$\hat{\mathcal{H}} = \omega_0 + v_{||}\hat{s}_0\left(\delta k_x\hat{\sigma}_x + \delta k_y\hat{\sigma}_y\right) + v_z\hat{s}_y\hat{\sigma}_z\delta k_z \pm m\hat{s}_z\hat{\sigma}_z$$

Jackiw-Rebbi-like surface states: $\Omega_\pm = \pm\sqrt{\zeta^2 + v_F^2\left(k_x^2 + k_y^2\right) + v_z^2 k_z^2}$

$\psi'^{(1)}_{s\pm} \sim iv_\perp k_z|e_1 + h_1 > +(v_{||}k_y - \Omega_{s\pm})|e_1 - h_1 >$

$${\psi'^{(1)}_{s\pm}}^\dagger \vec{s}\psi'^{(1)}_{s\pm} = \frac{v_\perp k_z}{\Omega_{s\pm}}\hat{y} + \frac{v_{||}k_y}{\Omega_{s\pm}}\hat{z}$$

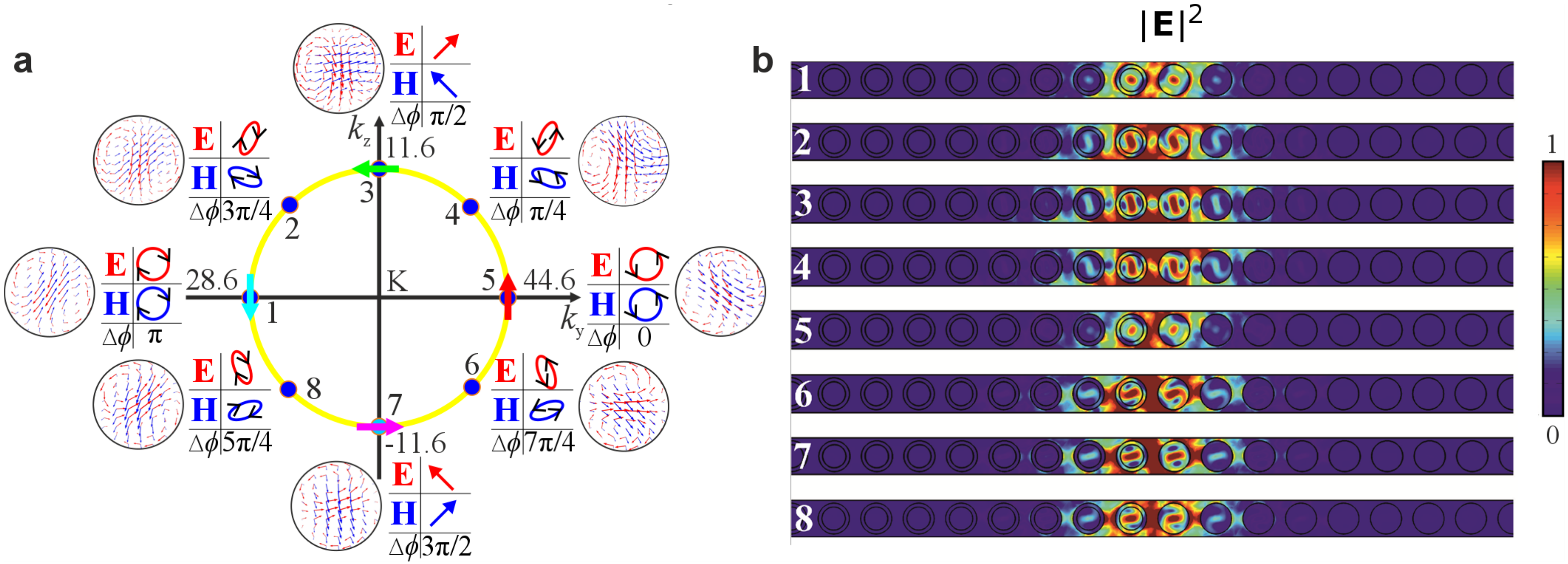

Topological robustness in three-dimensions

Reflectionless routing around sharp corners for out-of-plane ($k_z \neq 0$) propagation

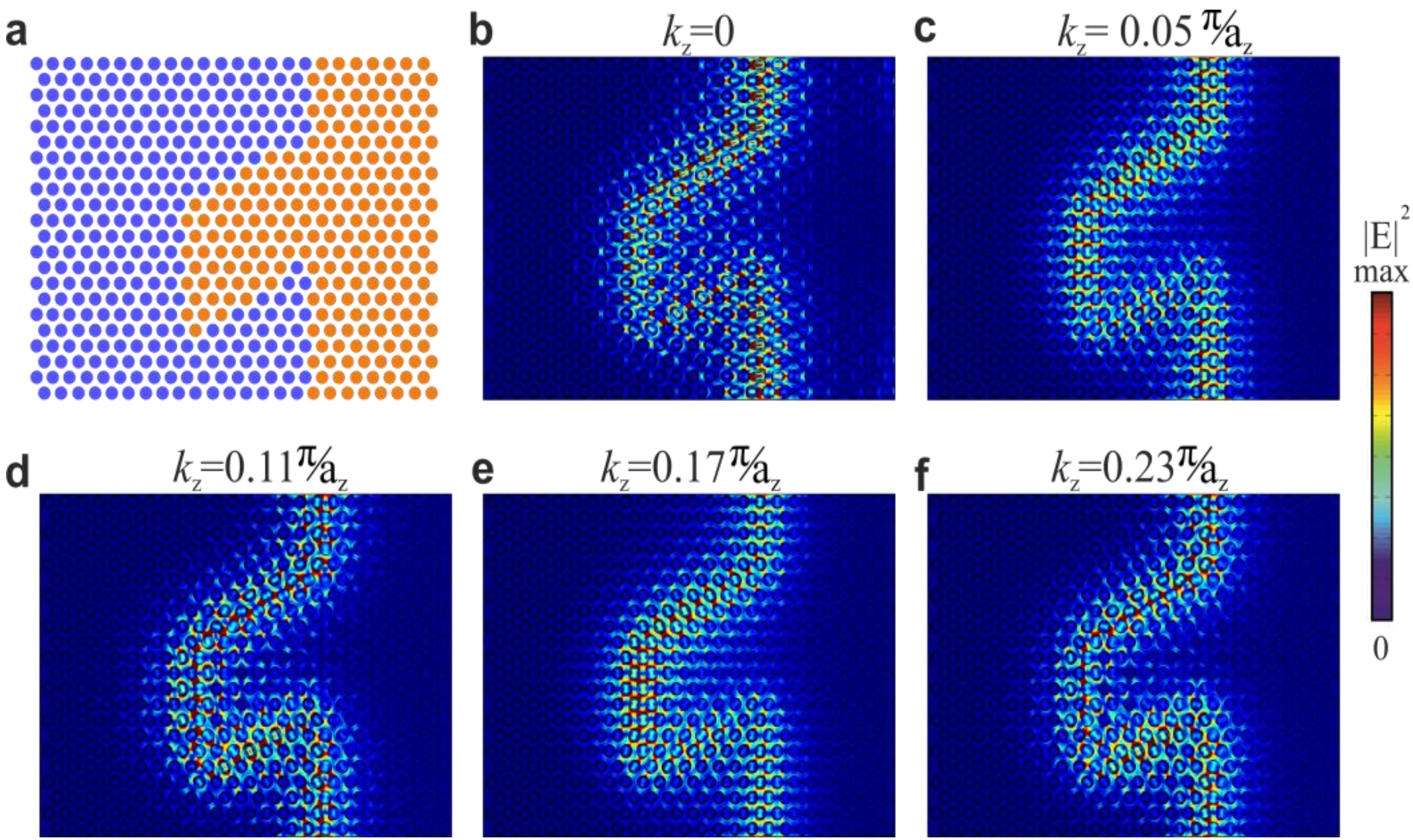

Vertical cut – non-topological interface

Non-topological surface states with Dirac point insured by the hexagonal symmetry of the defect

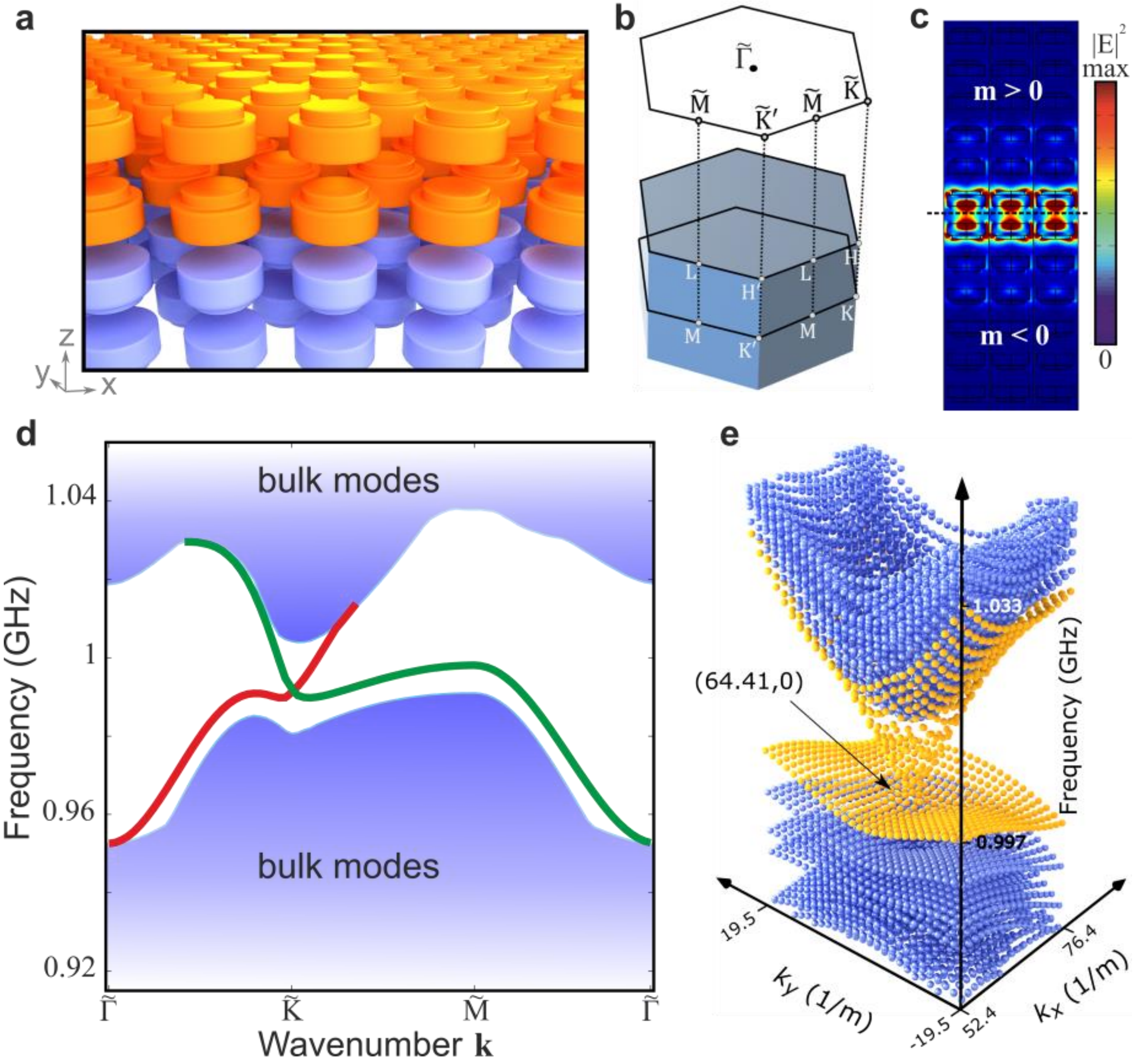

Acoustic and elastic topological states

1) Acoustic analogue of Quantum Hall effect

Nature Communications **6,** 8260, (2015).

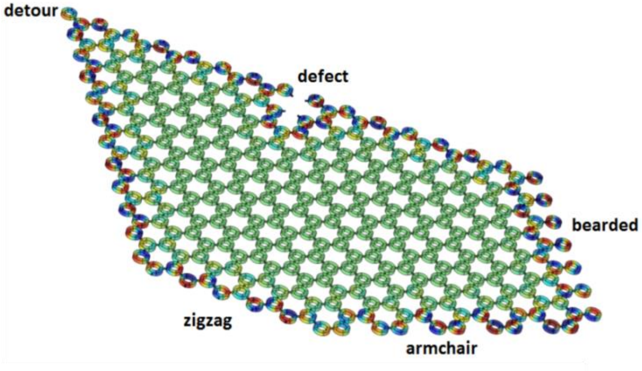

In collaboration with Andrea Alu (UT Austin)

2) Acoustic analogue of Quantum Spin Hall Effect

Nature Communications **6**, 8682 (2015).

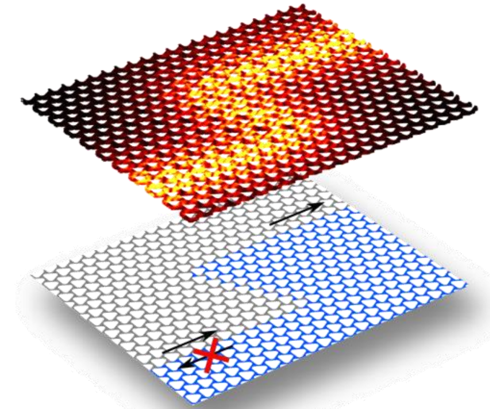

In collaboration with Hossein Mousavi and Zheng Wang (UT Austin)

3) Floquet Topological Insulators for Sound

Nature Communications **7**, 11744 (2016).

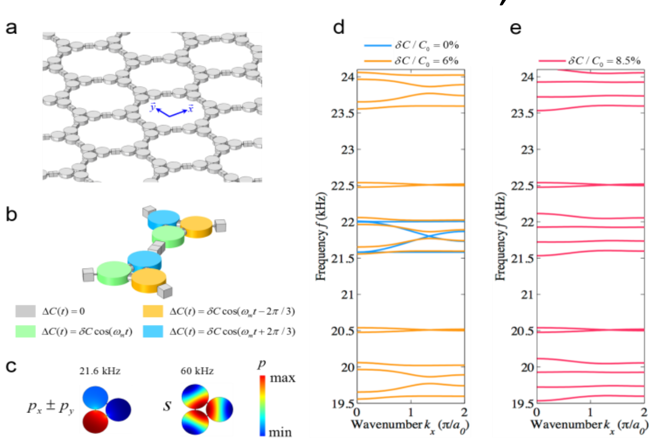

Emulating spin-orbit coupling and transition to phononic QSHE

Opening a counterbore breaks σ_z, while preserves in-plane symmetries.

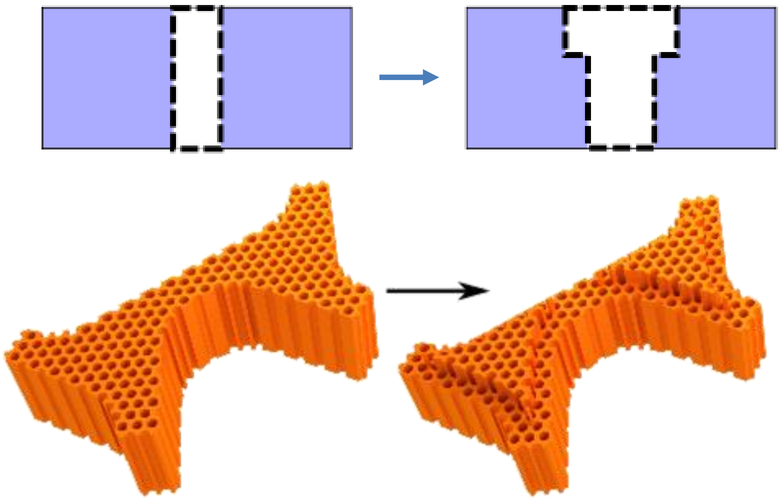

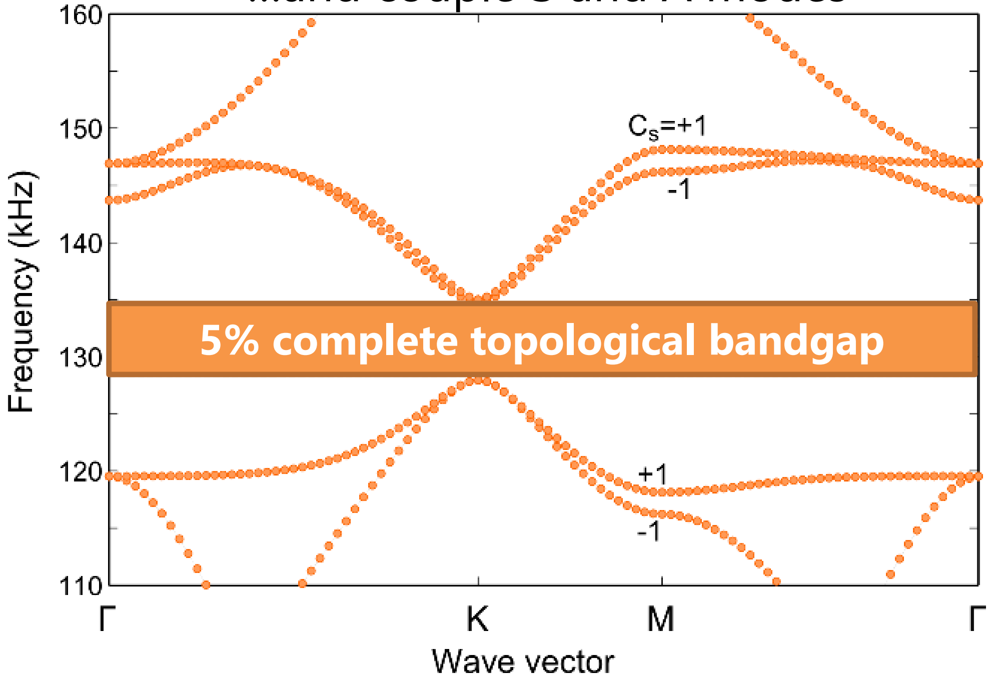

Berry curvature near K point:

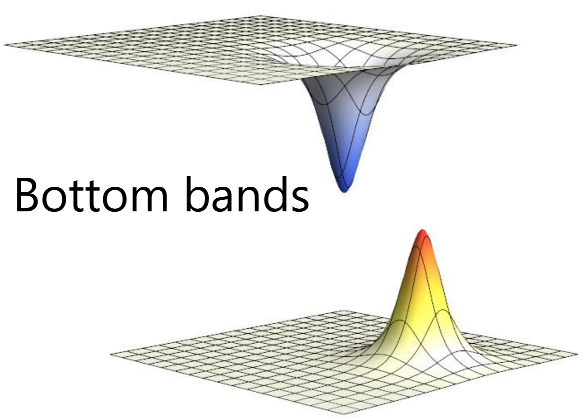

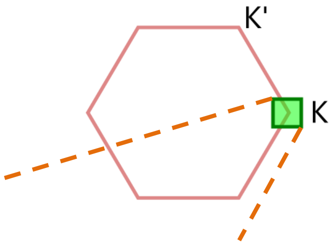

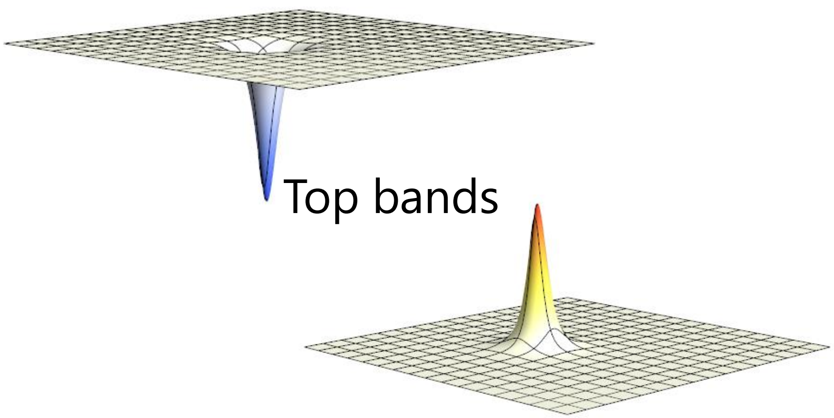

Topologically robust edge modes in Quantum Spin Hall Effect crystal

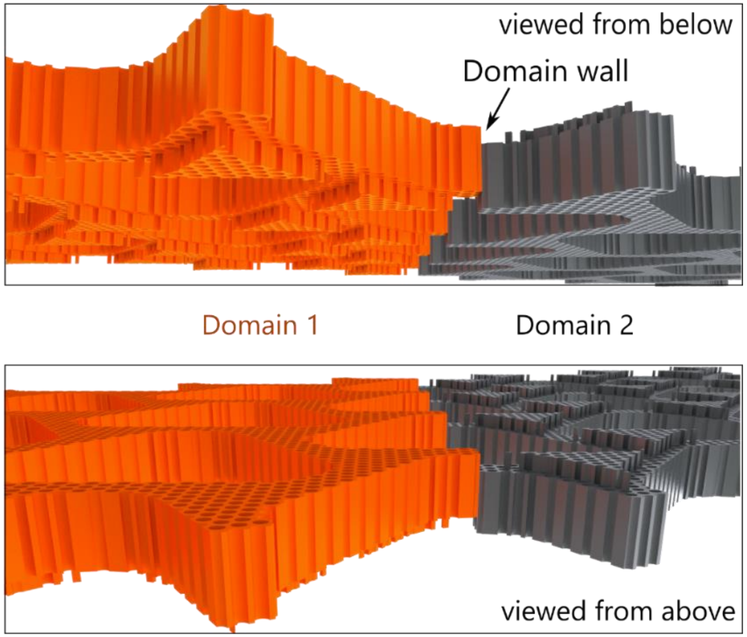

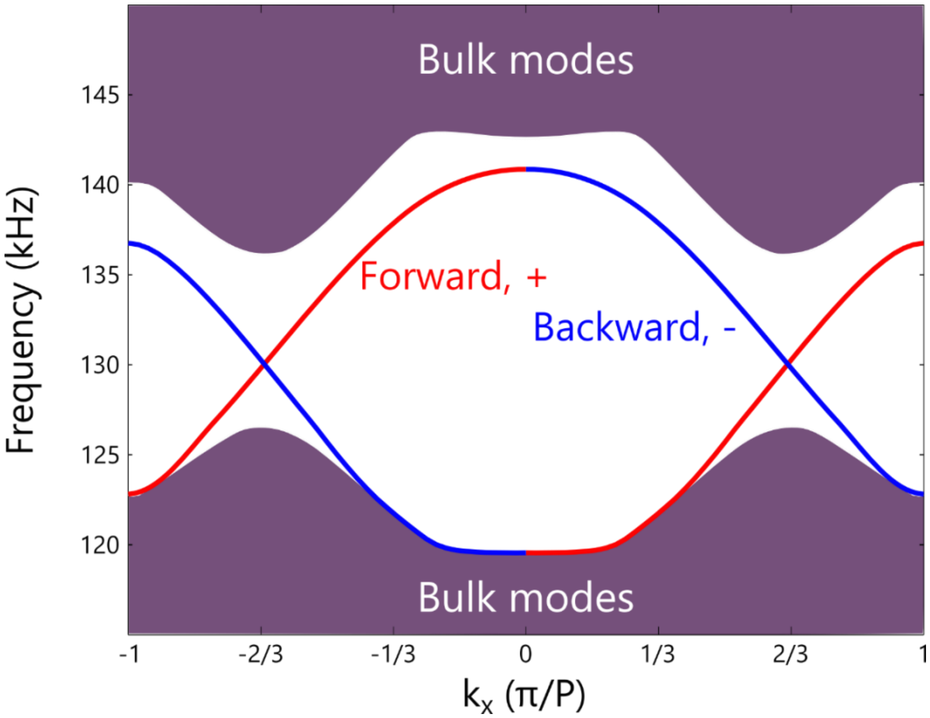

Massless helical edge states, spin locked to the propagation direction.

Time reversal operation changes the direction as well as the spin.

Trivial crystals are prone to defects and disorders

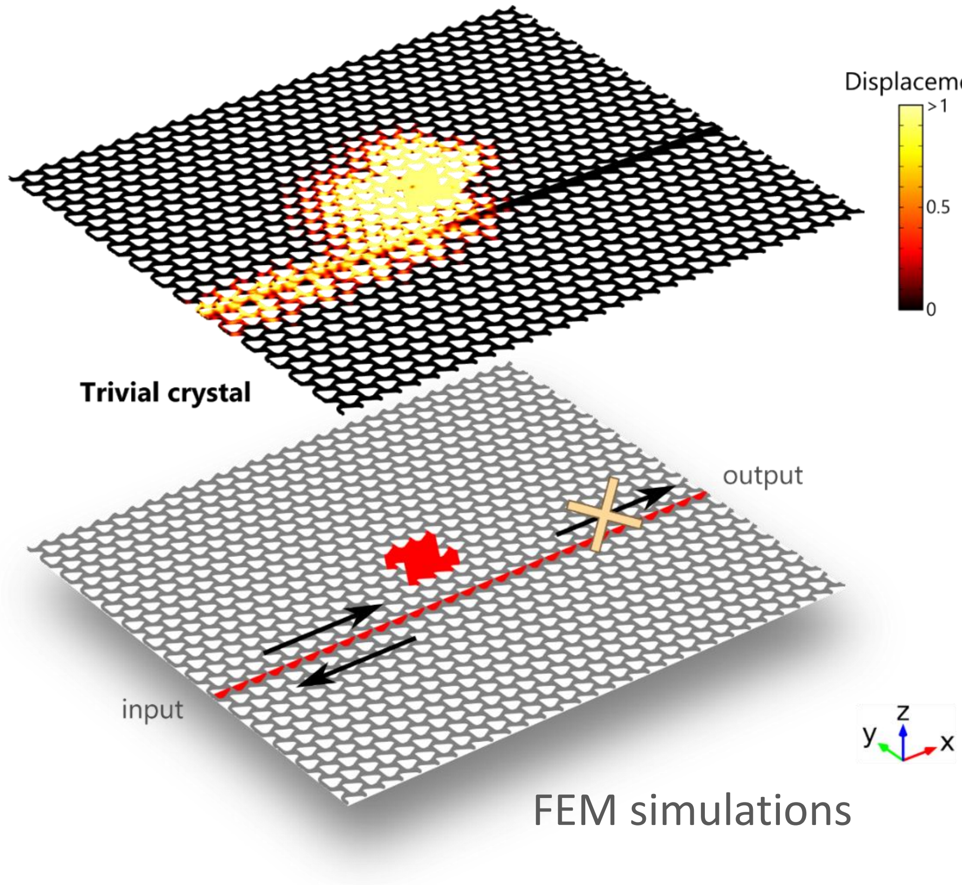

FEM simulations

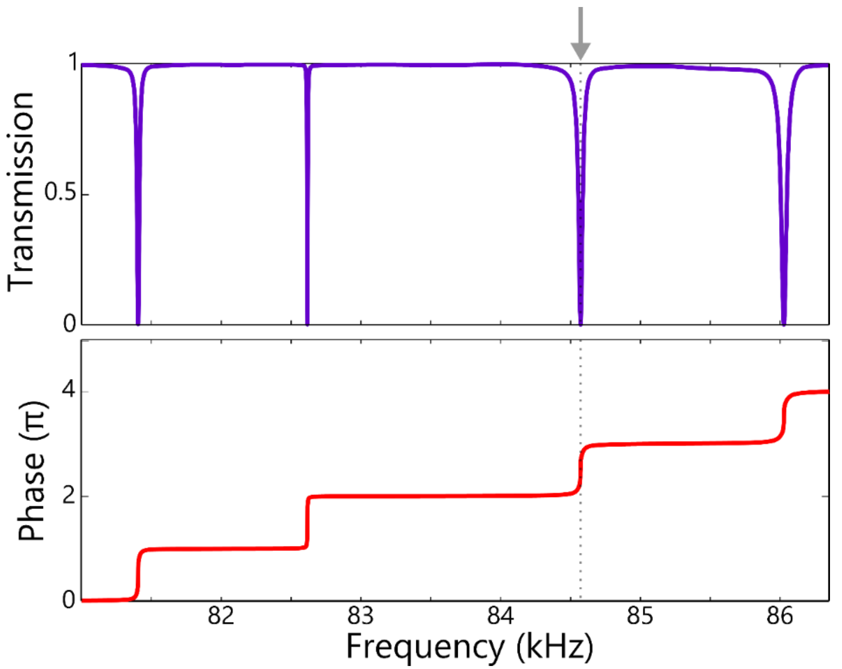

Each time a resonance occurs, phase changes by π and transmission drops to zero.

Robustness against defects and disorders in Quantum Spin Hall Effect crystal

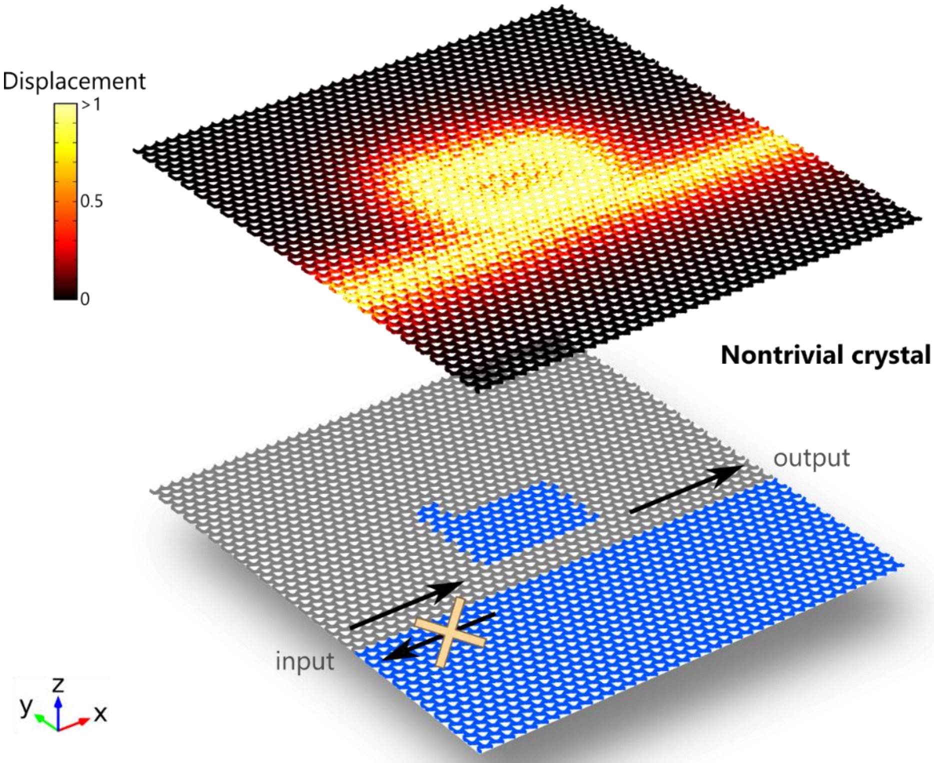

FEM simulations

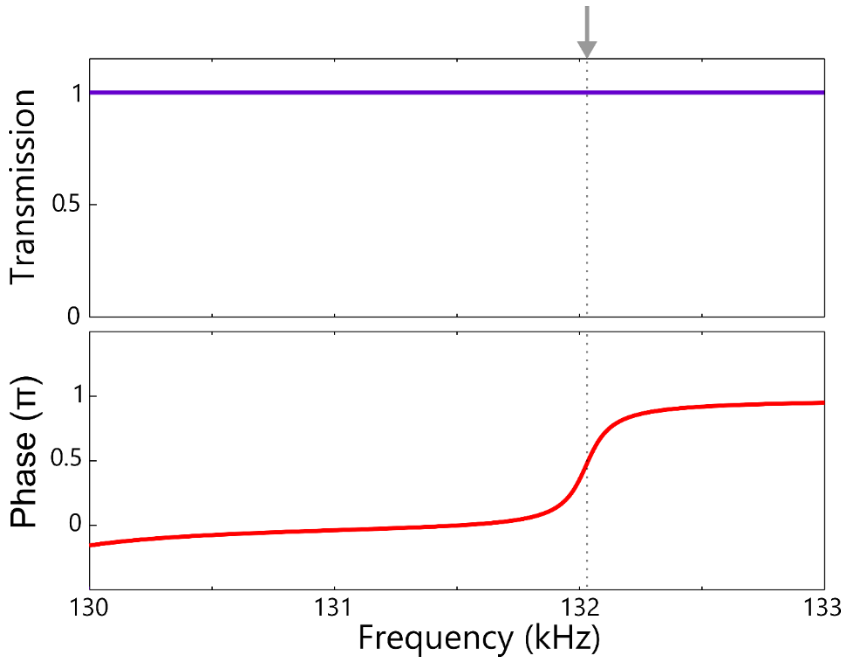

Resonance manifests itself only in the **phase!**

Robustness against sharp bends and rerouting in Quantum Spin Hall Effect crystal

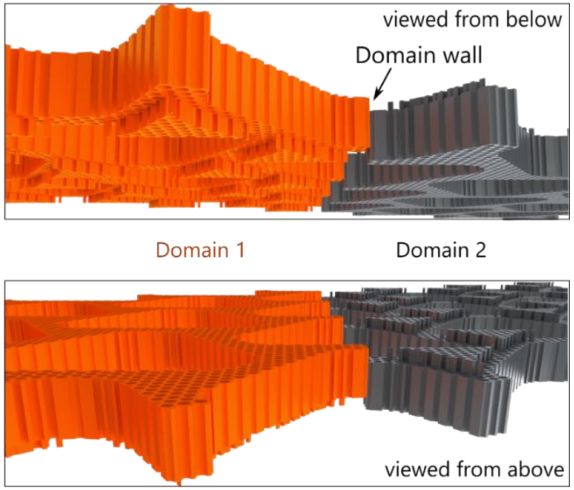

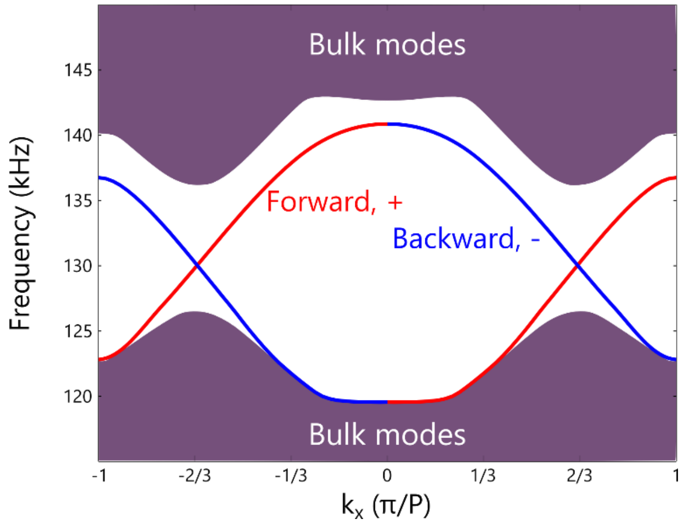

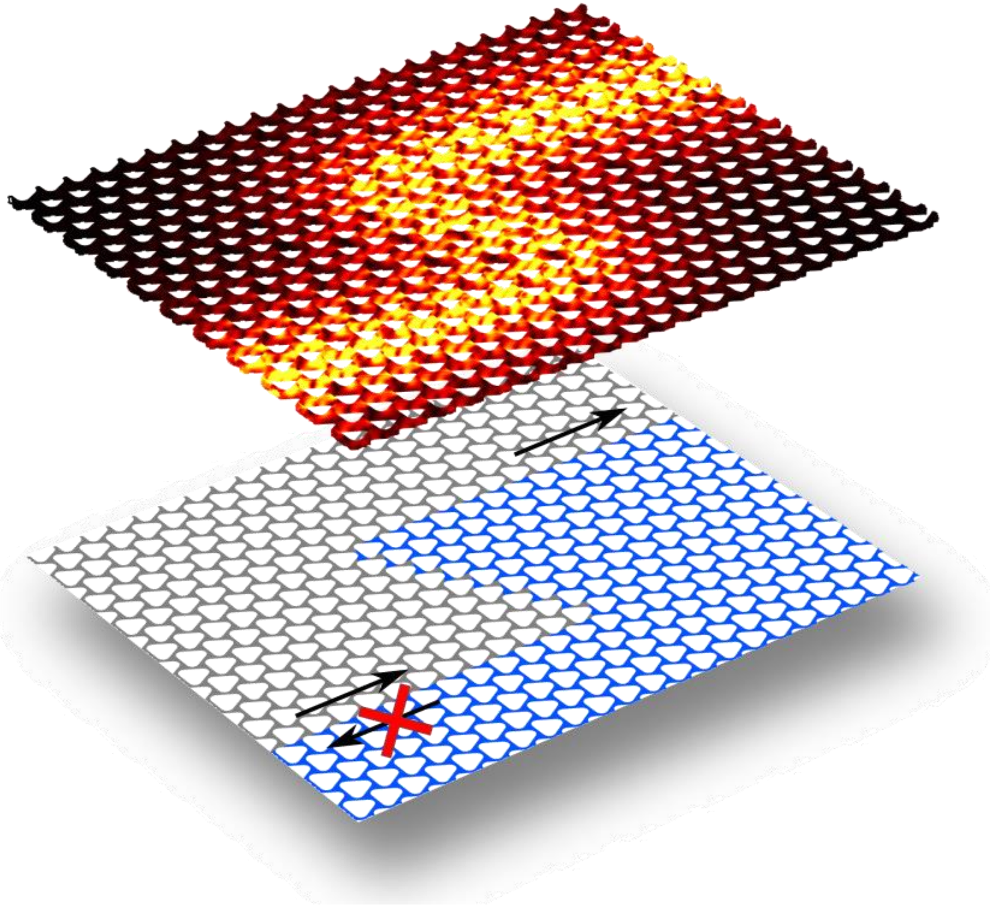

Summary and Outlook

- Photonic and acoustic systems offer an ideal platform for emulating topological states of condensed matter and quantum relativistic systems.
- Topological edge states envision a broad range of applications such as reconfigurable waveguides with controllable routing along the domain walls, and integrated optical systems where interaction among optical elements has "one-way" character.

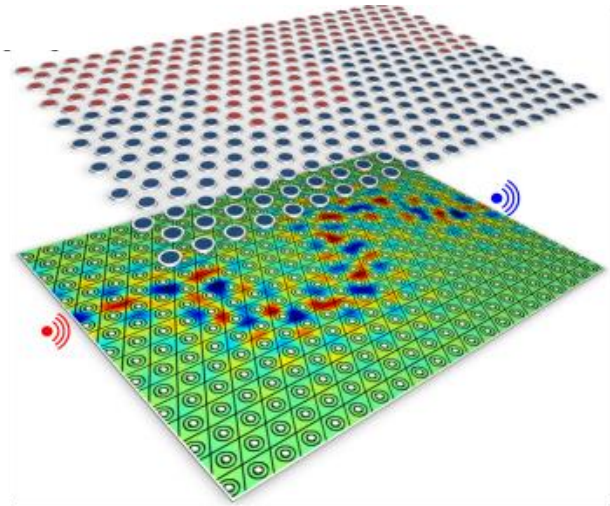

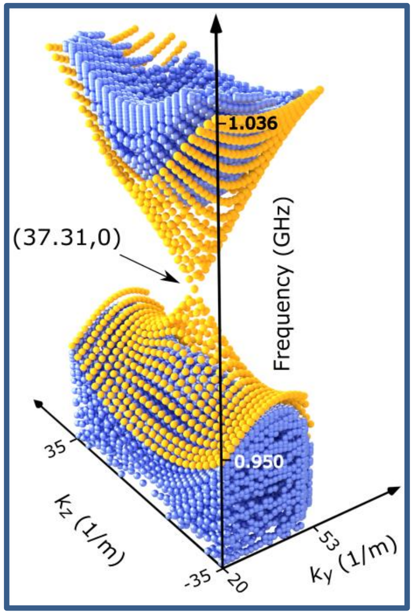

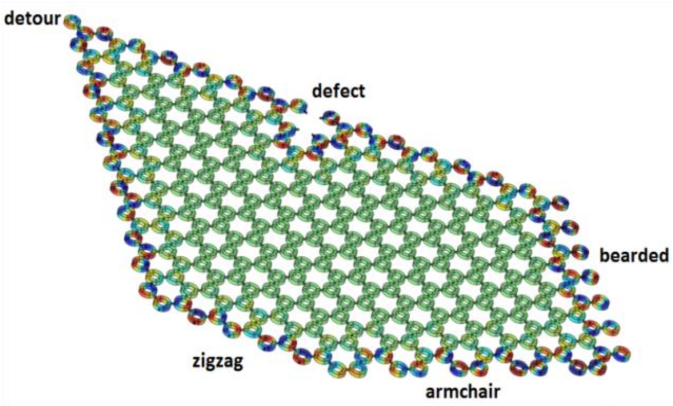

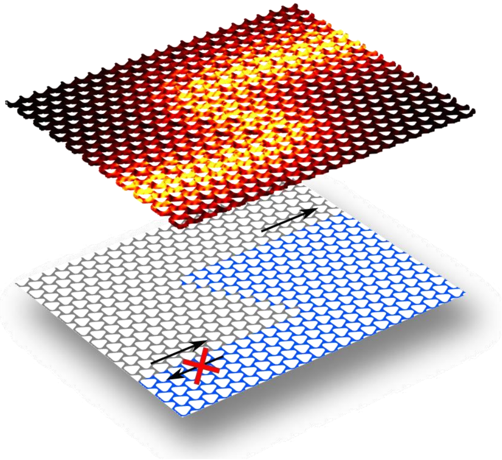

Thank you!

Research sponsored by National Science Foundation (USA)

CMMI-1537294 and EFRI-1641069